AFRL-SN-HS-TR-2004-045

SCATTERING-MATRIX ANALYSIS OF LINEAR PERIODIC ARRAYS OF SHORT ELECTRIC DIPOLES

Dr. Robert Shore
Dr. Arthur D. Yaghjian
Antenna Technology Branch
Electromagnetics Technology Division

In-House Technical Report: January 2002 – March 2004

APPROVED FOR PUBLIC RELEASE

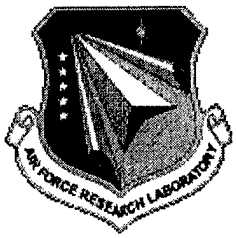

AIR FORCE RESEARCH LABORATORY
Sensors Directorate
Electromagnetics Technology Division
80 Scott Drive
Hanscom AFB MA 01731-2909

TECHNICAL REPORT

Scattering-Matrix Analysis of Linear Periodic Arrays of Short Electric Dipoles

Unlimited, Statement A

NOTICE

USING GOVERNMENT DRAWINGS, SPECIFICATIONS, OR OTHER DATA INCLUDED IN THIS DOCUMENT FOR ANY PURPOSE OTHER THAN GOVERNMENT PROCUREMENT DOES NOT IN ANY WAY OBLIGATE THE US GOVERNMENT. THE FACT THAT THE GOVERNMENT FORMULATED OR SUPPLIED THE DRAWINGS, SPECIFICATIONS, OR OTHER DATA DOES NOT LICENSE THE HOLDER OR ANY OTHER PERSON OR CORPORATION; OR CONVEY ANY RIGHTS OR PERMISSION TO MANUFACTURE, USE, OR SELL ANY PATENTED INVENTION THAT MAY RELATE TO THEM.

THIS TECHNICAL REPORT HAS BEEN REVIEWED AND IS APPROVED FOR PUBLICATION.

//Signature//

Robert Shore
Project Manager, Antenna Technology Branch

//Signature//

Livio Poles
Chief, Antenna Technology Branch

//Signature//

Michael N. Alexander
Technical Adivsor
Electromagnetics Technology Division

REPORT DOCUMENTATION PAGE

Form Approved
OMB No. 0704-0188

1. REPORT DATE *(DD-MM-YYYY)*		3. DATES COVERED *(From - To)*
25-04-2003	IN-HOUSE	15 January 2002 – 14 March 2004

4. TITLE AND SUBTITLE
SCATTERING-MATRIX ANALYSIS OF LINEAR PERIODIC ARRAYS OF SHORT ELECTRIC DIPOLES

5a. CONTRACT NUMBER

5b. GRANT NUMBER

5c. PROGRAM ELEMENT NUMBER
61102F

6. AUTHOR(S)
Robert A. Shore and Arthur D. Yaghjian

5d. PROJECT NUMBER
2304

5e. TASK NUMBER
HE

5f. WORK UNIT NUMBER
01

7. PERFORMING ORGANIZATION NAME(S) AND ADDRESS(ES)
AFRL/SNHA
80 Scott Drive
Hanscom AFB, MA 01731-2909

8. PERFORMING ORGANIZATION REPORT

9. SPONSORING / MONITORING AGENCY NAME(S) AND ADDRESS(ES)
Electromagnetics Technology Division
Sensors Directorate
Air Force Research Laboratory
80 Scott Drive
Hanscom AFB MA 01731-2909

10. SPONSOR/MONITOR'S ACRONYM(S)
AFRL/SNHA

11. SPONSOR/MONITOR'S REPORT NUMBER(S)

12. DISTRIBUTION / AVAILABILITY STATEMENT
Approved for public release; distribution unlimited. 22 June 2004, ESC 04-0653

13. SUPPLEMENTARY NOTES

14. ABSTRACT

The scattering-matrix analysis of linear periodic arrays of electric dipoles given in this report was suggested by the corresponding analysis performed by Yaghjian for linear periodic arrays of electro-acoustic monopole transducers. The extension to electromagnetic antennas reported here requires the use of the more complicated vector spherical wave functions instead of scalar spherical wave functions. However, no new concepts are needed for our treatment. A general vector spherical-wave source scattering-matrix description of electromagnetic antennas is formulated, and reciprocity and power conservation are used to derive relations between the antenna reflection, receiving and scattering coefficients that constitute the scattering matrix. When the antennas are electrically small dipoles only two vector spherical wave modes, one incoming and one outgoing, are required to describe the antennas. The scattering matrix formulation is applied to analyze infinite and finite linear periodic arrays of short electric dipoles perpendicular to the array axis. For an infinite periodic linear array of short dipoles, the scattering-matrix analysis leads to a simple implicit transcendental equation for the propagation constant β of the traveling wave in terms of the normalized separation distance kd and the phase ψ_e of the effective scattering coefficient of the array elements. Interestingly, for certain values of ψ_e and kd there can be two different values of β. The normalized separation distance and phase of the effective scattering coefficient also prove to be the only critical variables in the $N \times N$ matrix equation for the N radiation coefficients that is derived for a finite linear array of N electric dipoles. Resonances in the curves of total power radiated versus kd for a finite array excited with one feed element demonstrate the existence of the traveling waves predicted for the corresponding infinite array. These computed power curves, as well as directivity patterns, illustrate that the finite array becomes a more efficient endfire radiator as β approaches k. We also confirm that the maximum attainable endfire directivity of a finite array with a single feed element is a monotonically increasing function of the phase velocity of the traveling wave. The analysis of infinite linear periodic arrays is also extended to linear periodic arrays of short electric dipoles aligned with, and skew to, the array axis.

15. SUBJECT TERMS
Linear arrays, scattering matrices, traveling-wave antennas, electric dipoles.

16. SECURITY CLASSIFICATION OF:			17.LIMITATION OF ABSTRACT	18.NUMBER OF PAGES	19a. NAME OF RESPONSIBLE PERSON Robert A. Shore
a. REPORT	b. ABSTRACT	c.THIS PAGE			19b. TELEPHONE NUMBER *(include area code)*
Unclassified	Unclassified	Unclassified	SAR	52	*781-377-2058*

Standard Form 298 (Rev. 8-98)
Prescribed by ANSI Std. Z39.18

Contents

List of Figures

ACKNOWLEDGEMENT

This work was supported by the U.S. Air Force Office of Scientific Research (AFOSR).

The authors wish to thank Dr. Steven R. Best and Teresa O'Donnell for performing the NEC calculations for this work.

1 INTRODUCTION

The qualitative behavior of a finite-length periodic array of small antennas or scatterers closely spaced along a straight line can be understood in terms of traveling waves, supported by the corresponding infinitely long periodic array, and the fields of the feed antenna element(s) of the array that are not converted to traveling waves [1]–[7]. Consider, for example, the linear array (shown in Figure 1) consisting of eight perfectly conducting "dipoles" each separated by a distance d along the z axis. The first dipole is fed by a sinusoidal wave with frequency ω and the other seven dipoles are shorted to form passive straight-wire scatterers. The feed dipole radiates time-harmonic ($e^{-i\omega t}, \omega > 0$) fields that are partially converted to a traveling wave with $e^{i\beta z}$ dependence for discrete values of z along the array separated by integer multiples of the interelement spacing d. (To simplify the discussion, assume a single traveling wave exists at the frequency ω.) The traveling wave propagates without decay in the positive z direction with the real propagation constant $\beta > 0$ that depends on frequency. If the electrical size of each element is small enough, the periodic array of elements can support only a slow traveling wave with phase velocity less than or equal to the speed of light such that $\beta \geq k$, where $k = \omega/c = 2\pi/\lambda$ is the free-space propagation constant, λ is the free-space wavelength, and c is the speed of light. Without loss of generality, we can assume that $\beta d \leq \pi$ because as βd becomes greater than π the traveling wave simply becomes a slow wave traveling in the opposite direction.[1] Therefore, βd satisfies the inequalities

$$kd \leq \beta d \leq \pi \tag{1}$$

which imply that a traveling wave can exist only if the separation distance between the electrically small elements is less than or equal to half the traveling-wave wavelength, which is always less than or equal to free-space wavelength λ; therefore ($d \leq \lambda/2$). A proof of the inequalities in (1) for a general linear periodic array of lossless passive small elements is given in Appendix A where it is also shown that the fields of a nonradiating traveling wave on a linear infinite periodic array must decay exponentially with radial distance from the axis of the array.

The traveling wave excited by the feed element in Figure 1 propagates in the positive z direction and diffracts from the right end of the array much like a surface wave (or waveguide mode) diffracts from the end of a dielectric rod (or open-ended waveguide) [8], [9]. Part of the traveling wave is reflected and part is radiated unconfined by the array. The reflected traveling wave, which has $e^{-i\beta z}$ dependence, travels the length of the array and diffracts from the left end of the array in Figure 1. Again part of the traveling wave is reflected and part is radiated. This process of reflection and radiation from the ends of the array continues ad infinitum.

If the propagation constant β of the traveling wave is appreciably greater than the free-space propagation constant k, the traveling wave is strongly attached to the array elements, the impedance mismatch of the traveling wave as it encounters free space at the ends of the array will be large, and an appreciable amount of power in the incident traveling wave will

[1] If the elements of the array are highly dispersive, it is possible for the direction of power flow in the traveling wave to remain in the $+z$ direction for $\beta > \pi d$. If we then change this positive β to $-\beta'$ (for example, if $\pi/d < \beta < 2\pi/d$ let $\beta' = 2\pi/d - \beta < \pi/d$), the traveling wave is called a "backward traveling wave" [6, pp. 264, 341-349].

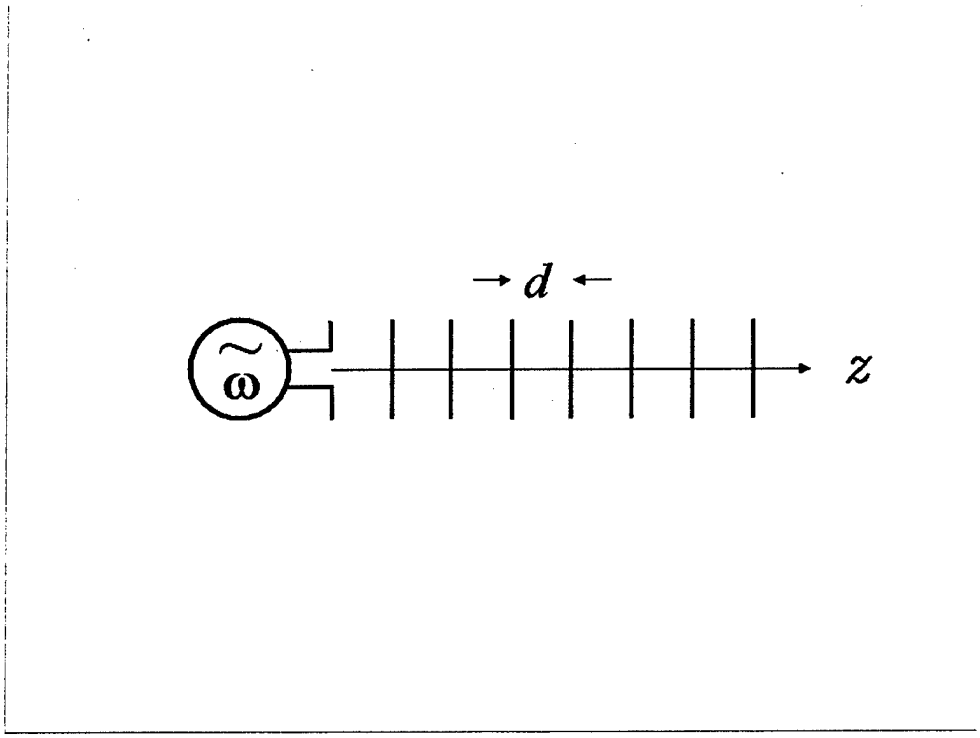

Figure 1: Linear periodic array of eight perfectly conducting dipoles separated by a distance d along the z axis and fed by a sinusoidal source with frequency ω.

be reflected. The array will then support a large standing wave at each kd value for which the phase of the traveling wave changes by an integer multiple of 360° as the traveling wave starts at one end of the array, travels the length of the array, reflects from the other end of the array, returns back, and reflects from the starting end of the array. The traveling wave will interfere constructively near these kd values and destructively well away from these values. Therefore, resonances will appear in the plots of total power radiated by the array (or, equivalently, total power accepted by the feed element of the array) versus kd. As the value of β gets closer to the value of k, the traveling wave becomes more weakly attached to the array elements and is launched more efficiently from the ends of the array so that the resonances caused by the constructive and destructive interference of the traveling wave become less pronounced. Moreover, as the value of β becomes closer to that of k, the significant fields of the traveling wave extend an increasingly further radial distance from the axis of the array. Therefore, the effective endfire aperture and endfire directivity of the array will increase as β gets closer in value to k (similar to the increase in effective aperture and directivity of the HE_{11} surface wave launched from the end of a dielectric rod [8]), until β gets so close in value to k and the traveling wave so broad that it cannot be efficiently excited by feeding one or more of the elements. If each element of the array is a small resonant antenna (or scatterer) with a narrow frequency band when it radiates (or scatters) alone in free space, this single element resonance will be superposed on the resonances of the traveling wave [10].

The resonances of the traveling wave will disappear for kd greater than the value at which the amplitude and phase of the coupling between the array elements will no longer support a traveling wave. (According to (1), this value is always less than or equal to π for small array elements.) For kd greater than this value, the induced excitation of each passive element diminishes rapidly with increasing distance from the feed element to the passive element, and the periodic array no longer radiates as an "endfire" antenna.

The foregoing qualitative description of the operation of linear periodic arrays can be partly gleaned and partly surmised from the experimental, theoretical, and numerical investigations into dipole (Yagi-Uda) arrays, as exemplified in the references [1]–[7]. It is not surprising that these previous investigations were limited to dipole arrays in which the number of dipoles, their spacing, and their dimensions did not vary over a wide range. The accurate construction of a variety of linear arrays and the accurate measurement of their near and far fields require an extremely tedious and time consuming experimental effort [1]. Purely theoretical analyses of linear arrays have been limited to obtaining approximate solutions to integral equations for infinite dipole arrays [2], [11]. Although numerical solutions to approximate integral equations have been successful for analyzing finite arrays [3], [4], [5], they become unwieldy for determining the effects of unrestricted changes in the array parameters, especially in large arrays. Even for a small array, an accurate numerical solution to the integral equations is very difficult to obtain if the individual elements of the array are resonant antennas or scatterers [10]. Moreover, the numerical difficulties increase if the elements of the array do not lie in a straight line, such as in closed-loop arrays [12], or if the elements are distributed over a surface or throughout a volume.

The scattering-matrix analysis of linear periodic arrays of electric dipoles given in this report was suggested by the corresponding analysis performed by Yaghjian [13] for linear periodic arrays of electroacoustic monopole transducers. The basic ideas of this report were

worked out by Yaghjian within the simpler analytic framework of scalar spherical wave functions. The extension to electromagnetic antennas reported here requires the use of the more complicated vector spherical wave functions. However, no new concepts are needed for our treatment of electromagnetic antennas. In this report we formulate a general vector spherical-wave scattering-matrix representation of antennas and derive reciprocity and lossless power conservation relations between the antenna reflection, receiving, transmitting, and scattering coefficients that constitute the scattering matrix. We then assume that each array element is an electrically small dipole antenna. This specialization of the general framework to small electric dipole antennas considerably simplifies the source scattering-matrix analysis since only two vector spherical wave modes (one incoming and one outgoing) are required to describe the antennas. The scattering matrix involves the receiving, transmitting, and scattering coefficients of each antenna element, as well as the input reflection coefficient of the waveguide mode feeding each antenna. However, for a linear periodic array, the reciprocity and lossless power conservation relations reduce the critical scattering-matrix variables in the N equations for the N unknown outgoing wave coefficients of the array elements to one single parameter, the phase of the effective scattering coefficient of each antenna element. (The number of elements N and the normalized spacing kd of the elements in the linear periodic array are the other critical variables in the equations.)

The magnitude of this effective scattering coefficient does not enter the equations because reciprocity and power conservation demand that the magnitude $|S_e|$ and phase ψ_e of the effective scattering coefficient ($S_e = |S_e|e^{i\psi_e}$) satisfy the simple relationship

$$|S_e| = \frac{3}{2}\sin\psi_e \tag{2}$$

which implies that $0 \leq \psi_e \leq \pi$ and that ψ_e approaches 0 or π as the magnitude of the scattering coefficient approaches zero. We also prove regardless of reciprocity and power conservation relations that an infinite linear periodic array of short electric dipole antennas oriented perpendicular to the array axis can support a nondecaying traveling wave only if the relationship (2) is satisfied. Remarkably, in contrast with the acoustic monopole case, it is possible to have two traveling waves for each value of ψ_e. A simple implicit transcendental equation determines the $kd - \beta d$ diagram for these traveling waves. The theoretical propagation velocity of the traveling wave supported by a periodic array of short thin wires obtained from the $kd - \beta d$ diagram in combination with values of the effective scattering coefficient of the wires calculated using the NEC computer code [26] are shown to compare well with the measurements of Ehrenspeck and Poehler [1] for the case of Yagi-Uda arrays.

All of the properties exhibited by finite linear periodic arrays explained in the first part of this introduction are clearly and conveniently demonstrated by solving the $N \times N$ matrix equation for these arrays as the value of the phase ψ_e of the effective scattering coefficient is varied from 0 to π and the value of kd ranges from 0 to π (that is, over the range of kd at which a traveling wave can exist). In addition, we confirm the result, found experimentally by Ehrenspeck and Poehler [1] and predicted theoretically by Hansen and Woodyard [14], that the maximum endfire directivity attainable by varying the number of elements in a linear periodic array of electrically small elements supporting a single traveling wave (and having one feed element) depends only on (and increases monotonically with) the relative

phase velocity of the traveling wave.

The remainder of the paper is divided into eight main sections in addition to the Concluding Remarks (Section 10) and the Appendices. The reader interested in just the equations and results for linear periodic arrays of small electric dipoles oriented perpendicular to the array axis, and not in how they are derived, can concentrate on Sections 6 and 7, which discuss infinite and finite arrays, respectively. Section 2 introduces the basic field equations and the vector spherical-wave source scattering-matrix description of a general electromagnetic antenna system. Sections 3 and 4 derive reciprocity and lossless power relations, respectively, that must be satisfied by the coefficients of the scattering matrix of a general linear, reciprocal, lossless antenna. Section 5 applies these reciprocity and power relations to the small electric dipoles that are used in Sections 6 and 7 for the analysis of infinite and finite arrays of dipoles oriented perpendicular to the array axis. Sections 8 and 9 consider arrays of dipoles aligned with, and skew to, the array axis.

2 SOURCE SCATTERING-MATRIX DESCRIPTION OF A GENERAL ANTENNA

The electromagnetic system under consideration is pictured in Figure 2. The antenna is bounded by the closed surface A_T. The electromagnetic power supply or detector is bounded by the closed surface A_P and the power supply feeds the antenna through a waveguide with reference plane A_0 common to both A_T and A_P. The power supply sends time-harmonic $(e^{-i\omega t}, \omega > 0)$ electromagnetic power down the waveguide in the form of a single propagating waveguide mode. (The waveguide is assumed to be composed of perfect conductors separated by a linear, homogeneous, isotropic medium.) The antenna converts the electromagnetic fields of the waveguide mode into time-harmonic electromagnetic fields that propagate in the free space in which the antenna and its power supply or detector are placed. The space between the spherical reference surface A_r with radius r and the external surface $A_E = (A_T - A_0) + (A_P - A_0)$ of the antenna plus power supply or detector contains no electromagnetic sources, although arbitrary time-harmonic electromagnetic sources at frequency ω, such as other antennas, may exist outside A_r. It is assumed that the external part of the surface of the power supply or detector $(A_P - A_0)$ is electromagnetically shielded so that no electromagnetic power crosses $(A_P - A_0)$.

The Maxwell equations that govern the time-harmonic electromagnetic fields in the source-free free space between the surface A_E and the spherical surface A_r are [15, sec. 7.1]

$$\nabla \times \mathbf{E}(\mathbf{r}) = ikZ_0\mathbf{H} \tag{3a}$$

$$\nabla \times \mathbf{H}(\mathbf{r}) = -ik\mathbf{E}(\mathbf{r})/Z_0 \tag{3b}$$

which imply that for $k \neq 0$

$$\nabla \cdot \mathbf{E}(\mathbf{r}) = 0 \tag{3c}$$

$$\nabla \cdot \mathbf{H}(\mathbf{r}) = 0 \tag{3d}$$

where $\mathbf{E}(\mathbf{r})$ and $\mathbf{H}(\mathbf{r})$ are the electric and magnetic fields, Z_0 is the free space impedance, $k = \omega/c = 2\pi/\lambda$ is the free space propagation constant, λ is the free-space wavelength, and

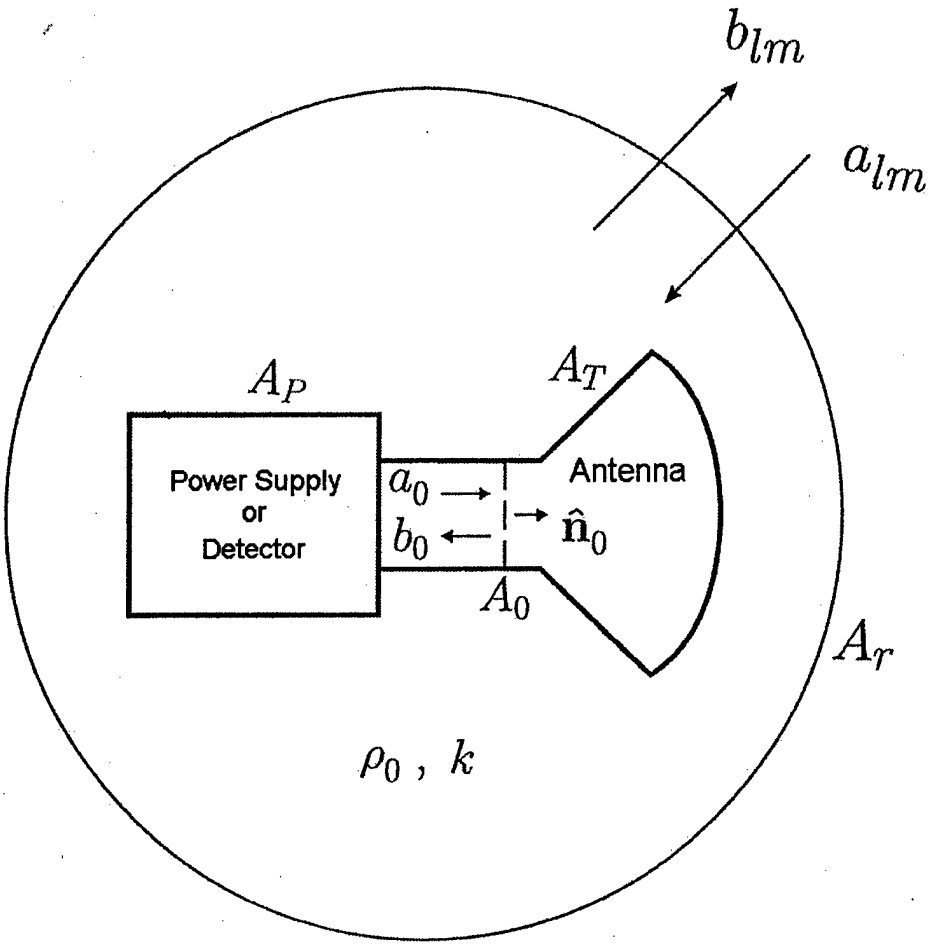

Figure 2: Schematic of the electromagnetic antenna system. The external surface of the power supply or detector is given by $A_E = (A_T - A_0) + (A_P - A_0)$.

c is the speed of light. Eliminating either $\mathbf{H}(\mathbf{r})$ or $\mathbf{E}(\mathbf{r})$ from the Maxwell equations (3a) and (3c) yields the vector wave equations

$$-\nabla \times \nabla \times \mathbf{E}(\mathbf{r}) + k^2\,\mathbf{E}(\mathbf{r}) = 0 \tag{4a}$$

$$-\nabla \times \nabla \times \mathbf{H}(\mathbf{r}) + k^2\,\mathbf{H}(\mathbf{r}) = 0 \tag{4b}$$

which imply

$$\nabla^2\mathbf{E}(\mathbf{r}) + k^2\,\mathbf{E}(\mathbf{r}) = 0, \quad \nabla \cdot \mathbf{E}(\mathbf{r}) = 0 \tag{5a}$$

$$\nabla^2\mathbf{H}(\mathbf{r}) + k^2\,\mathbf{H}(\mathbf{r}) = 0, \quad \nabla \cdot \mathbf{H}(\mathbf{r}) = 0. \tag{5b}$$

Since the electric field satisfies (5a) across the surface A_r (which lies within free space), the electric field on the surface can be expanded in a complete set of divergenceless vector spherical wave functions [15],[16]

$$\mathbf{E}(\mathbf{r}) = \sum_{l=1}^{\infty}\sum_{m=-l}^{l}\left[a_{lm}^{(1)}\mathbf{M}_{lm}^{(1)}(\mathbf{r}) + b_{lm}^{(1)}\mathbf{M}_{lm}^{(2)}(\mathbf{r}) + a_{lm}^{(2)}\mathbf{N}_{lm}^{(1)}(\mathbf{r}) + b_{lm}^{(2)}\mathbf{N}_{lm}^{(2)}(\mathbf{r})\right]. \tag{6}$$

The spherical-wave expansion of the magnetic field then follows from (3a)

$$\mathbf{H}(\mathbf{r}) = -\mathrm{i}Y_0\sum_{l=1}^{\infty}\sum_{m=-l}^{l}\left[a_{lm}^{(1)}\mathbf{N}_{lm}^{(1)}(\mathbf{r}) + b_{lm}^{(1)}\mathbf{N}_{lm}^{(2)}(\mathbf{r}) + a_{lm}^{(2)}\mathbf{M}_{lm}^{(1)}(\mathbf{r}) + b_{lm}^{(2)}\mathbf{M}_{lm}^{(2)}(\mathbf{r})\right], \tag{7}$$

where $Y_0 = 1/Z_0$ is the free-space admittance. The vector spherical harmonics $\mathbf{M}_{lm}^{(i)}(\mathbf{r})$ and $\mathbf{N}_{lm}^{(i)}(\mathbf{r})$ are defined in Appendix B. The $\mathbf{M}_{lm}^{(i)}(\mathbf{r})$ spherical wave functions have no radial component. Because of that the $\mathbf{M}_{lm}^{(i)}(\mathbf{r})$ functions in (6) and the $\mathbf{N}_{lm}^{(i)}(\mathbf{r})$ functions in (7) are often referred to as TE waves while the $\mathbf{N}_{lm}^{(i)}(\mathbf{r})$ functions in (6) and the $\mathbf{M}_{lm}^{(i)}(\mathbf{r})$ functions in (7) are often referred to as TM waves; they satisfy the equations

$$\mathbf{N}_{lm}^{(i)}(\mathbf{r}) = \frac{1}{k}\nabla \times \mathbf{M}_{lm}^{(i)}(\mathbf{r}) \tag{8a}$$

$$\mathbf{M}_{lm}^{(i)}(\mathbf{r}) = \frac{1}{k}\nabla \times \mathbf{N}_{lm}^{(i)}(\mathbf{r}). \tag{8b}$$

The $\mathbf{M}_{lm}^{(1)}(\mathbf{r})$ and $\mathbf{N}_{lm}^{(1)}(\mathbf{r})$ have the radial dependence $j_l(kr)$ while the $\mathbf{M}_{lm}^{(2)}(\mathbf{r})$ and $\mathbf{N}_{lm}^{(2)}(\mathbf{r})$ have the radial dependence $h_l^{(1)}(kr)$ where $j_l(kr)$ and $h_l^{(1)}(kr)$ are the spherical Bessel functions and the spherical Hankel functions of the first kind, respectively. The expansions in (6) and (7) are known as multipole expansions. The $l = 1$ terms are the dipole terms, the $l = 2$ terms are the quadrupole terms, etc. The summations containing the modal coefficients $a_{lm}^{(i)}$ in (6) and (7) equal the electromagnetic fields produced by the sources (applied and induced) that reside outside the surface A_r. The summations containing the modal coefficients $b_{lm}^{(i)}$ in (6) and (7) equal the electromagnetic fields produced by the sources (applied and induced) that reside inside the surface A_r or, equivalently, inside the external surface A_E of the antenna plus power supply or detector. They are the fields radiated and scattered by the antenna and its power supply or detector.

The tangential electric and magnetic fields $[\mathbf{E}_{tan}(\boldsymbol{\rho}), \mathbf{H}_{tan}(\boldsymbol{\rho})]$ on the reference plane A_0 of the feed waveguide can be written in terms of the electric and magnetic basis fields $[\mathbf{e}_0(\boldsymbol{\rho}), \mathbf{h}_0(\boldsymbol{\rho})]$ of the single propagating waveguide mode with incident amplitude a_0 and emergent amplitude b_0; specifically

$$\mathbf{E}_{tan}(\boldsymbol{\rho}) = V_0 \mathbf{e}_0(\boldsymbol{\rho}), \quad \mathbf{H}_{tan}(\boldsymbol{\rho}) = I_0 \mathbf{h}_0(\boldsymbol{\rho}) \tag{9}$$

where

$$V_0 = a_0 + b_0, \quad I_0 = \eta_0(a_0 - b_0). \tag{10}$$

There may be evanescent modes in the feed waveguide, but the fields of these evanescent modes are assumed to be negligible on the reference plane A_0.

If the dimensional units of $\mathbf{e}_0$ and $\mathbf{h}_0$ are chosen as $(\text{meter})^{-1}$ and they are consistent with Maxwell's equations in the International System of mksA units, then V_0 has units of Volts, I_0 has units of Amperes, and the characteristic admittance η_0 of the waveguide can be chosen as a real positive constant with units of $(\text{Ohm})^{-1}$. It then follows that normalization of the basis fields may be expressed as a nondimensional number equal to one, that is

$$\int_{A_0} [\mathbf{e}_0(\boldsymbol{\rho}) \times \mathbf{h}_0(\boldsymbol{\rho})] \cdot \hat{\mathbf{n}}_0 dA = 1 \tag{11}$$

where $\hat{\mathbf{n}}_0$ is the inward normal to the antenna on the plane A_0. If the plane A_0 simply cuts two wire leads at quasi-static frequencies, V_0 and I_0 refer to conventional circuit voltages and currents that do not serve as genuine modal coefficients. In that case, the equations in (10) become definitions of a_0 and b_0 such that

$$a_0 \equiv (V_0 + I_0/\eta_0)/2, \quad b_0 \equiv (V_0 - I_0/\eta_0)/2. \tag{12}$$

The "outgoing" modal coefficients $(b_0, b_{lm}^{(i)})$ of the antenna system are related to the "incoming" modal coefficients $(a_0, a_{lm}^{(i)})$ of the antenna system by a linear matrix transformation termed the "source scattering-matrix equations" [17], [18] for the spherical-wave representation of the antenna. These source scattering-matrix equations can be written as

$$b_0 = \Gamma a_0 + \sum_{l=1}^{\infty} \sum_{m=-l}^{l} \sum_{s=1}^{2} R_{lm}^{(s)} a_{lm}^{(s)} \tag{13}$$

$$b_{lm}^{(s)} = T_{lm}^{(s)} a_0 + \sum_{l'=1}^{\infty} \sum_{m'=-l'}^{l'} \sum_{s'=1}^{2} S_{lm;l'm'}^{(s),(s')} a_{l'm'}^{(s')}. \tag{14}$$

The coefficients $R_{lm}^{(s)}$, $T_{lm}^{(s)}$, and $S_{lm;l'm'}^{(s),(s')}$ in the source scattering matrix embody the receiving, transmitting, and scattering properties of the linear antenna. The complex number Γ is the reflection coefficient (phase referenced to the plane A_0) of the waveguide mode and equals b_0/a_0 when all sources outside the external surface A_E of the antenna and its power supply are zero, in other words, when there are no sources outside A_r so that all the a_{lm}^s equal zero.

The spherical-wave source scattering matrix given in (13)–(14) for electromagnetic antennas differs from the classical spherical-wave scattering-matrix given in [19, secs. 9.18–9.24]

because the classical scattering matrix uses $(h_l^{(2)}, h_l^{(1)})$ radial basis functions in (6) and (7) instead of $(j_l, h_l^{(1)})$. This small mathematical change from $h_l^{(2)}$ to j_l appreciably simplifies the analysis by relating all the scattering-matrix coefficients directly to the physical sources. For example, if an antenna with its power supply or detector does not scatter fields produced by external sources, then the source scattering coefficients $S_{lm;l'm'}^{(s),(s')}$ are equal to zero. This is not the case for the classical spherical-wave scattering-matrix description of antennas [20, sec. 2.3.5].

Finally, note that for a scatterer rather than an antenna, we can set $T_{lm}^{(s)}$ and $R_{lm}^{(s)}$ equal to zero and equation (13) becomes superfluous.

3 RECIPROCITY RELATIONS

The receiving, transmitting, and scattering coefficients in the source scattering matrix for antennas composed entirely of reciprocal material must satisfy reciprocity relations that can be derived from the following electromagnetic reciprocity theorem [21, sect. 1.9]

$$\int_{A_0} [\mathbf{E}_2(\boldsymbol{\rho}) \times \mathbf{H}_1(\boldsymbol{\rho}) - \mathbf{E}_1(\boldsymbol{\rho}) \times \mathbf{H}_2(\boldsymbol{\rho})] \cdot \hat{\mathbf{n}}_0 dA = \int_{A_r} [\mathbf{E}_2(\mathbf{r}) \times \mathbf{H}_1(\mathbf{r}) - \mathbf{E}_1(\mathbf{r}) \times \mathbf{H}_2(\mathbf{r})] \cdot \hat{\mathbf{n}} dA \tag{15}$$

where $[\mathbf{E}_1(\boldsymbol{\rho}), \mathbf{H}_1(\boldsymbol{\rho}), \mathbf{E}_1(\mathbf{r}), \mathbf{H}_1(\mathbf{r})]$ and $[\mathbf{E}_2(\boldsymbol{\rho}), \mathbf{H}_2(\boldsymbol{\rho}), \mathbf{E}_2(\mathbf{r}), \mathbf{H}_2(\mathbf{r})]$ are the fields of the antenna excited by any two sets of electromagnetic sources located inside the power supply or outside the spherical surface A_r.

Substituting the electric and magnetic fields on A_0 in the waveguide from (9)–(10) into the left-hand side (LHS) of (15), and then using the integral relation (11) we find that the LHS of (15) is equal to

$$2\eta_0 \left(b_{2_0} a_{1_0} - b_{1_0} a_{2_0} \right). \tag{16}$$

Substituting the electric and magnetic fields on A_r from (6) and (7) and using the orthogonality relations [20, Eq. A1.71] (see (124),(125))

$$\int_0^{2\pi} \int_0^{\pi} \left[\mathbf{M}_{lm}^{(i)}(\mathbf{r}) \times \mathbf{M}_{\lambda\mu}^{(j)}(\mathbf{r}) \right] \cdot \hat{\mathbf{r}} \sin\theta d\theta d\phi = 0 \tag{17a}$$

$$\int_0^{2\pi} \int_0^{\pi} \left[\mathbf{N}_{lm}^{(i)}(\mathbf{r}) \times \mathbf{N}_{\lambda\mu}^{(j)}(\mathbf{r}) \right] \cdot \hat{\mathbf{r}} \sin\theta d\theta d\phi = 0 \tag{17b}$$

we see that all integrals of cross-products involving $\mathbf{M}_{lm}^{(i)}(\mathbf{r}) \times \mathbf{M}_{\lambda\mu}^{(j)}(\mathbf{r})$ and $\mathbf{N}_{lm}^{(i)}(\mathbf{r}) \times \mathbf{N}_{\lambda\mu}^{(j)}(\mathbf{r})$ can be set equal to zero. If, in addition, we make use of the reciprocity integral relations [20, Eqs. A1.72-A1.74] (see (124),(125))

$$\int_S \left[\mathbf{M}_{lm}^{(i)}(\mathbf{r}) \times \mathbf{N}_{\lambda\mu}^{(j)}(\mathbf{r}) - \mathbf{M}_{\lambda\mu}^{(j)}(\mathbf{r}) \times \mathbf{N}_{lm}^{(i)}(\mathbf{r}) \right] \cdot d\mathbf{S} = \delta_{l\lambda} \delta_{m,-\mu} \frac{(-1)^{m+1}}{k^2} A^{(i,j)} \tag{18a}$$

$$\int_S \left[\mathbf{N}_{lm}^{(i)}(\mathbf{r}) \times \mathbf{M}_{\lambda\mu}^{(j)}(\mathbf{r}) - \mathbf{N}_{\lambda\mu}^{(j)}(\mathbf{r}) \times \mathbf{M}_{lm}^{(i)}(\mathbf{r})\right] \cdot d\mathbf{S} = \delta_{l\lambda}\delta_{m,-\mu} \frac{(-1)^{m+1}}{k^2} A^{(i,j)} \tag{18b}$$

where $A^{(1,1)} = 0, A^{(1,2)} = \mathrm{i}, A^{(2,1)} = -\mathrm{i}, A^{(2,2)} = 0$ and the surface of integration in (18a) and (18b) is a spherical surface S of radius r with outward area element $d\mathbf{S} = \hat{\mathbf{r}} r^2 \sin\theta d\theta d\phi$, we find that the right-hand side (RHS) of (15) is equal to

$$\frac{Y_0}{k^2} \sum_{l=1}^{\infty} \sum_{m=-l}^{l} (-1)^{m+1} \left[a_{2;lm}^{(1)} b_{1;l,-m}^{(1)} - b_{2;l,m}^{(1)} a_{1;l,-m}^{(1)} + a_{2;lm}^{(2)} b_{1;l,-m}^{(2)} - b_{2;l,m}^{(2)} a_{2;l,-m}^{(2)}\right] \tag{19}$$

Letting $\sum_{lms} \equiv \sum_{l=1}^{\infty} \sum_{m=-l}^{l} \sum_{s=1}^{2}$ and equating (16) with (19) we obtain

$$2\eta_0 \left(b_{2_0} a_{1_0} - b_{1_0} a_{2_0}\right) = \frac{Y_0}{k^2} \sum_{lms} (-1)^{m+1} \left[a_{2;lm}^{(s)} b_{1;l,-m}^{(s)} - b_{2;l,m}^{(s)} a_{1;l,-m}^{(s)}\right]. \tag{20}$$

Substituting expressions for $b_{2_0}, b_{1_0}, b_{1;l,-m}^{(s)}$, and $b_{2;l,m}^{(s)}$ from the source scattering-matrix equations (13) and (14), the equation (20) becomes

$$\begin{aligned} a_{1_0} \sum_{lms} \left[2\eta_0 R_{lm}^{(s)} - \frac{(-1)^{m+1} Y_0}{k^2} T_{l,-m}^{(s)}\right] a_{2;lm}^{(s)} - a_{2_0} \sum_{lms} \left[2\eta_0 R_{lm}^{(s)} - \frac{(-1)^{m+1} Y_0}{k^2} T_{l,-m}^{(s)}\right] a_{1;lm}^{(s)} \\ - \frac{Y_0}{k^2} \sum_{lms} \sum_{l'm's'} a_{2;lm}^{(s)} (-1)^{m+1} S_{l,-m;l'm'}^{(s),(s')} a_{1;l'm'}^{(s')} \\ + \frac{Y_0}{k^2} \sum_{lms} \sum_{l'm's'} a_{1;l,-m}^{(s)} (-1)^{m+1} S_{l,m;l'm'}^{(s),(s')} a_{2;l'm'}^{(s')} = 0. \end{aligned} \tag{21}$$

By rewriting the indices of the fourth term we then obtain

$$\begin{aligned} a_{1_0} \sum_{lms} \left[2\eta_0 R_{lm}^{(s)} - \frac{(-1)^{m+1} Y_0}{k^2} T_{l,-m}^{(s)}\right] a_{2;lm}^{(s)} - a_{2_0} \sum_{lms} \left[2\eta_0 R_{lm}^{(s)} - \frac{(-1)^{m+1} Y_0}{k^2} T_{l,-m}^{(s)}\right] a_{1;lm}^{(s)} \\ - \frac{Y_0}{k^2} \sum_{lms} \sum_{l'm's'} a_{2;lm}^{(s)} \left[(-1)^{m+1} S_{l,-m;l'm'}^{(s),(s')} - (-1)^{m'+1} S_{l',-m';lm}^{(s'),(s)}\right] a_{1;l'm'}^{(s')} = 0. \end{aligned} \tag{22}$$

Since the modal coefficients a_{1_0} and a_{2_0} are determined by the power supply connected to the waveguide, and the modal coefficients $a_{1_{lm}}^{(s)}$ and $a_{2_{lm}}^{(s)}$ are determined by the sources outside A_r, they can all be chosen independently. Therefore (22) can hold for all values of the modal coefficients if and only if the quantities in each of the sets of square brackets are zero. Specifically, the receiving, transmitting, and scattering coefficients of the source scattering matrix must satisfy the reciprocity relations

$$2\eta_0 R_{lm}^{(s)} = \frac{(-1)^{m+1} Y_0}{k^2} T_{l,-m}^{(s)} \tag{23}$$

$$(-1)^m S_{l,-m;l'm'}^{(s),(s')} = (-1)^{m'} S_{l',-m';lm}^{(s'),(s)}. \tag{24}$$

The reciprocity relation (23) states that the spherical-wave receiving coefficients of an antenna containing only reciprocal material are equal to a constant times the spherical-wave

transmitting coefficients. The reciprocity relation (24) states that the fields scattered into one outgoing spherical mode, when another spherical mode is incident upon the antenna, remain the same if the mode numbers of the incident and outgoing modes are interchanged. For a scatterer rather than an antenna, $T_{lm}^{(s)} = R_{lm}^{(s)} = 0$ and only the reciprocity relation (24) is relevant.

4 POWER CONSERVATION RELATIONS

Conservation of power also places restrictions upon the coefficients of the scattering matrix. If the antennas are lossless, the net average power flowing across the reference plane A_0 of the waveguide toward the antenna must equal the net average power flowing out of the spherical surface A_r. Mathematically, this conservation of average power flow can be expressed from Poynting's theorem as

$$\frac{1}{2}\mathrm{Re}\int_{A_0}[\mathbf{E}_{tan}(\boldsymbol{\rho})\times\mathbf{H}_{tan}^{*}(\boldsymbol{\rho})]\cdot\hat{\mathbf{n}}_0 dA = \frac{1}{2}\mathrm{Re}\int_{A_r}[\mathbf{E}(\mathbf{r})\times\mathbf{H}^{*}(\mathbf{r})]\cdot d\mathbf{S}. \tag{25}$$

Inserting $\mathbf{E}_{tan}(\boldsymbol{\rho})$ and $\mathbf{H}_{tan}(\boldsymbol{\rho})$ from (9)–(10) into the left hand side of (25), and then using the integral relation (11) the LHS of (25) is found to equal

$$\frac{1}{2}\eta_0\left(|a_0|^2 - |b_0|^2\right) \tag{26}$$

To evaluate the RHS of (25) we begin by substituting the vector spherical wave function expansions of $\mathbf{E}(\mathbf{r})$ and $\mathbf{H}(\mathbf{r})$ given by (6) and (7). We then use the orthogonality relations [16, Eqs.VI-7,VI-8] together with [15, Eq.9.121], and [16, Eqs.VI-6,VI-7] together with [15, Eq.9-120], along with the Wronskian formulas for spherical Bessel and Hankel functions to show that the RHS of (25) is equal to

$$\frac{1}{2k^2}Y_0\sum_{lms}\left[|b_{lm}^{(s)}|^2 + \mathrm{Re}\left(b_{lm}^{(s)}a_{lm}^{(s)*}\right)\right]. \tag{27}$$

Equating (26) and (27) we obtain the conservation of power relation

$$\frac{1}{2}\eta_0\left(|a_0|^2 - |b_0|^2\right) = \frac{1}{2k^2}Y_0\sum_{lms}\left[|b_{lm}^{(s)}|^2 + \mathrm{Re}\left(b_{lm}^{(s)}a_{lm}^{(s)*}\right)\right]. \tag{28}$$

If the antenna neither radiates nor scatters, the $b_{lm}^{(s)}$ modal coefficients would all be zero and the net average power crossing the sphere A_r would be zero, even though the $a_{lm}^{(s)}$ modal coefficients generated by electromagnetic sources outside A_r may not be zero. In that case, the average power entering the surface A_r would equal the average power leaving. With the right hand side of (28) zero, the left hand side must also be zero for this lossless antenna, and all the power in the waveguide mode propagating toward the antenna is reflected back down the waveguide ($|b_0|^2 = |a_0|^2$).

When the b_0 and $b_{lm}^{(s)}$ modal coefficients from the source scattering-matrix equations (13) and (14) are substituted into (28), this equation can be written as

$$|a_0|^2 \left[\frac{\eta_0 k^2}{Y_0} \left(1 - |\Gamma|^2 \right) - \sum_{lms} \left| T_{lm}^{(s)} \right|^2 \right]$$

$$- \left[\frac{\eta_0 k^2}{Y_0} \left| \sum_{lms} R_{lm}^{(s)} a_{lm}^{(s)} \right|^2 + \sum_{lms} \left(\left| \sum_{l'm's'} S_{lm;l'm'}^{(s),(s')} a_{l'm'}^{(s')} \right|^2 + \mathrm{Re} \sum_{l'm's'} S_{lm;l'm'}^{(s),(s')} a_{l'm'}^{(s')} a_{lm}^{(s)*} \right) \right]$$

$$-2\mathrm{Re} \left[a_0 \sum_{lms} \left(\frac{\eta_0 k^2}{Y_0} \Gamma R_{lm}^{(s)*} a_{lm}^{(s)*} + \frac{1}{2} T_{lm}^{(s)} a_{lm}^{(s)*} + \sum_{l'm's'} T_{lm}^{(s)} S_{lm;l'm'}^{(s),(s')*} a_{l'm'}^{(s')*} \right) \right] = 0. \quad (29)$$

Because the modal coefficients a_0 and $a_{lm}^{(s)}$ can be chosen independently, let all the $a_{lm}^{(s)}$ equal zero to get from (29) the first power relation

$$\sum_{lms} \left| T_{lm}^{(s)} \right|^2 = \frac{\eta_0 k^2}{Y_0} \left(1 - |\Gamma|^2 \right). \quad (30)$$

Next, let $a_0 = 0$ to show that the quantity inside the second set of square brackets in (29) is zero. Since all but any one of the $a_{lm}^{(s)}$ can be chosen zero, the quantity in the second set of square brackets in (29) can vanish for all $a_{lm}^{(s)}$ only if

$$\mathrm{Re} \left(S_{lm;lm}^{(s),(s)} \right) + \sum_{l'm's'} \left| S_{l'm';lm}^{(s),(s')} \right|^2 = -\frac{\eta_0 k^2}{Y_0} \left| R_{lm}^{(s)} \right|^2. \quad (31)$$

Lastly, the quantity inside the third set of square brackets in (29) must be zero because the quantities inside the other two sets of square brackets are zero. All but one $a_0 a_{lm}^{(s)}$ at a time can be chosen zero and the one nonzero $a_0 a_{lm}^{(s)}$ can be given a purely real or purely imaginary value in order to reveal a third power relation

$$\frac{T_{lm}^{s}}{2} + \sum_{l'm's'} T_{l'm'}^{(s')} S_{lm;l'm'}^{(s'),(s)*} = -\frac{\eta_0 k^2}{Y_0} \Gamma R_{lm}^{(s)*}. \quad (32)$$

The power relation (30) expresses mathematically that, in the absence of exterior sources, the total power radiated by a lossless antenna equals the power supplied to the antenna through the waveguide. The power relation (31) implies that the total power received by a lossless antenna that is not transmitting can always be related to the scattering coefficients of the source scattering matrix. The power relation (32) shows that for lossless antennas the product of the reflection coefficient and each receiving coefficient of the source scattering matrix is linearly related to the corresponding transmitting coefficient and the sum of products of all the transmitting and scattering coefficients. This last power relation, which comes from the cross coupling terms in the quadratic power expression (29), has no immediately obvious physical interpretation.

For lossless scatterers rather than lossless antennas, $T_{lm}^{(s)} = R_{lm}^{(s)} = 0$ and $|\Gamma| = 1$ so that the power relations (30) and (32) vanish and (31) becomes

$$\mathrm{Re} \left(S_{lm;lm}^{(s),(s)} \right) + \sum_{l'm's'} \left| S_{l'm';lm}^{(s'),(s)} \right|^2 = 0. \quad (33)$$

5 SHORT Z DIRECTED ELECTRIC DIPOLES

We now specialize the general vector spherical wave expansions (6) and (7) and the source scattering-matrix equations (13) and (14) to the case of a short z directed electric dipole antenna. The electric and magnetic fields of an elementary electric (Hertzian) dipole antenna are proportional to $\mathbf{N}_{10}^{(2)}(\mathbf{r})$ and $-\mathrm{i}Y_0\mathbf{M}_{10}^{(2)}(\mathbf{r})$, respectively. Explicit expressions for these outgoing vector spherical waves are [16, pp. 40-41]

$$\mathbf{N}_{10}^{(2)}(\mathbf{r}) = \frac{\mathrm{i}h_1^{(1)}(kr)}{kr}\sqrt{\frac{3}{2\pi}}\cos\theta\hat{\mathbf{r}} - \mathrm{i}\frac{1}{kr}\frac{d}{d(kr)}\left[krh_1^{(1)}(kr)\right]\frac{1}{2}\sqrt{\frac{3}{2\pi}}\sin\theta\hat{\boldsymbol{\theta}}, \tag{34a}$$

$$-\mathrm{i}Y_0\mathbf{M}_{10}^{(2)}(\mathbf{r}) = Y_0h_1^{(1)}(kr)\frac{1}{2}\sqrt{\frac{3}{2\pi}}\sin\theta\hat{\boldsymbol{\phi}}. \tag{34b}$$

Substituting expressions for the spherical Hankel functions, we find the r and θ components of $\mathbf{N}_{10}^{(2)}(\mathbf{r})$ are given by

$$N_{10,r}^{(2)}(\mathbf{r}) = -\mathrm{i}\frac{\mathrm{e}^{\mathrm{i}kr}}{(kr)^2}\left(1+\frac{\mathrm{i}}{kr}\right)\sqrt{\frac{3}{2\pi}}\cos\theta \tag{35a}$$

$$N_{10,\theta}^{(2)}(\mathbf{r}) = -\frac{\mathrm{e}^{\mathrm{i}kr}}{kr}\left(1+\frac{\mathrm{i}}{kr}-\frac{1}{(kr)^2}\right)\frac{1}{2}\sqrt{\frac{3}{2\pi}}\sin\theta, \tag{35b}$$

and similarly

$$-\mathrm{i}Y_0M_{10,\phi}^{(2)}(\mathbf{r}) = -Y_0\frac{\mathrm{e}^{\mathrm{i}kr}}{kr}\left(1+\frac{\mathrm{i}}{kr}\right)\frac{1}{2}\sqrt{\frac{3}{2\pi}}\sin\theta. \tag{35c}$$

Equations (35a)-(35b) and (35c) are the components of the electric and magnetic fields, respectively, of a z directed electric point-current source (Hertzian dipole) [22, p. 436]. The electric fields incident upon the antenna from sources outside A_r are given by the incoming $\mathbf{N}_{lm}^{(1)}(\mathbf{r})$ and $\mathbf{M}_{lm}^{(1)}(\mathbf{r})$ terms in (6). If the dimensions of the antenna (and its power supply or detector) are appreciably smaller than a wavelength, and the origin of the coordinate system is centered on the antenna, the incident electric field over the region of space occupied by the antenna ($r \ll \lambda$) can be well approximated by just the $\mathbf{N}_{1m}^{(1)}(\mathbf{r})$ modes because the electric fields of all the other modes approach zero as kr approaches zero. Additionally, as kr approaches zero $\mathbf{N}_{1,\pm1}^{(1)}(\mathbf{r})$ have only an x and y electric-field component. Moreover, if we assume that the scattered fields of the electric dipole antenna are also electric dipole fields, (6) shows that the z component of the electric field just outside the antenna is given by

$$E_z(\mathbf{r}) = \left[a_{10}^{(2)}\mathbf{N}_{10}^{(1)}(\mathbf{r}) + b_{10}^{(2)}\mathbf{N}_{10}^{(2)}(\mathbf{r})\right]\cdot\hat{\mathbf{z}}, \qquad kr \ll 1 \tag{36}$$

which can be expanded as

$$E_z(\mathbf{r}) = a_{10}^{(2)}\mathrm{i}\frac{1}{3}\sqrt{\frac{3}{2\pi}} - b_{10}^{(2)}\sqrt{\frac{3}{2\pi}}\frac{\mathrm{e}^{\mathrm{i}kr}}{kr}\left[\mathrm{i}\left(\frac{1}{kr}+\frac{\mathrm{i}}{(kr)^2}\right)\cos\theta\hat{\mathbf{r}} + \frac{1}{2}\left(1+\frac{\mathrm{i}}{kr}-\frac{1}{(kr)^2}\right)\sin\theta\hat{\boldsymbol{\theta}}\right]\cdot\hat{\mathbf{z}}, \quad kr \ll 1. \tag{37}$$

If we let E_z^0 refer to the incident electric field at the center (origin) of the antenna, that is

$$E_z^0 = \mathrm{i}\sqrt{\frac{1}{6\pi}}a_{10}^{(2)} \tag{38}$$

and let b refer to the coefficient of the $\mathrm{e}^{\mathrm{i}kr}/(kr)$ radiated electric field, that is

$$b = \frac{1}{2}\sqrt{\frac{3}{2\pi}}b_{10}^{(2)} \tag{39}$$

(37) becomes

$$E_z(\mathbf{r}) = E_z^0 - b\frac{\mathrm{e}^{\mathrm{i}kr}}{kr}\left[2\mathrm{i}\left(\frac{1}{kr}+\frac{\mathrm{i}}{(kr)^2}\right)\cos\theta\hat{\mathbf{r}} + \left(1+\frac{i}{kr}-\frac{1}{(kr)^2}\right)\sin\theta\hat{\boldsymbol{\theta}}\right]\cdot\hat{\mathbf{z}},\quad kr << 1\,. \tag{40}$$

We note that the b-term in (40) that is dotted into $\hat{\mathbf{z}}$, which gives the electric field radiated and scattered by the small electric dipole antenna, holds for all kr outside the antenna.

Since all the $T_{lm}^{(s)}$ are zero except $T_{10}^{(2)}$ for an antenna that radiates as an electric dipole, the reciprocity relation (23) demands that all the $R_{lm}^{(s)}$ are zero except $R_{10}^{(2)}$. Also, with all the $b_{lm}^{(s)}$ and $T_{lm}^{(s)}$ zero except when $l=1, m=0$, and $s=2$, (14) and the reciprocity relation (24) imply that all the $S_{l'm';lm}^{(s),(s')}$ are zero except $S_{10;10}^{(2),(2)}$. Thus, the source scattering-matrix equations (13) and (14) for such an electrically small z directed dipole reduce to

$$b_0 = \Gamma a_0 + RE_z^o \tag{41}$$

$$b = Ta_0 + SE_z^o \tag{42}$$

in which the renormalized receiving, transmitting, and scattering coefficients for the small z directed electric dipole antenna are defined as

$$R = \frac{R_{10}^{(2)}}{\mathrm{i}\sqrt{\frac{1}{6\pi}}},\quad T = \frac{1}{2}\sqrt{\frac{3}{2\pi}}T_{10}^{(2)},\quad S = -\mathrm{i}\frac{3}{2}S_{10;10}^{(2),(2)}. \tag{43}$$

The reciprocity relation (24) reduces to an identity for the small z directed electric dipole, and the reciprocity relation (23) becomes

$$R = \mathrm{i}\frac{Y_0}{\eta_0}\frac{2\pi}{k^2}T. \tag{44}$$

The power relations (30)–(32) for the electrically small lossless z directed dipole simplify considerably to

$$|T|^2 = \frac{\eta_0 k^2}{Y_0 4\pi}\frac{3}{2}\left(1-|\Gamma|^2\right) \tag{45}$$

$$\mathrm{Im}\,(S) - \frac{2}{3}|S|^2 = \frac{\eta_0 k^2}{Y_0 4\pi}|R|^2 \tag{46}$$

$$T\left(\frac{1}{2}\mathrm{i}+\frac{2}{3}S^*\right) = -\frac{\eta_0\, k^2}{Y_0 4\pi}\Gamma R^*\,. \tag{47}$$

The reciprocity relation (44) can be used to eliminate R in (46) and (47), so that they can be written as

$$\mathrm{Im}\,(S) - \frac{2}{3}|S|^2 = \frac{Y_0\pi}{\eta_0 k^2}|T|^2 \tag{48}$$

$$T\left(\frac{1}{2}\mathrm{i} + \frac{2}{3}S^*\right) = \frac{1}{2}\mathrm{i}\Gamma T^* \,. \tag{49}$$

Taking the absolute value and then squaring both sides of (49) produces (48) after $|T|^2$ is substituted from (45) . Therefore, (48) is redundant, and we are left with three independent equations obtained from the reciprocity and power conservation relations for a small, reciprocal, lossless z directed electric dipole antenna, namely equations (44), (45), and (49).

Writing T in (44) and (49) as $|T|\mathrm{e}^{\mathrm{i}\psi_T}$ shows that the transmitting, receiving, and scattering coefficients can be expressed merely in terms of the reflection coefficient $\Gamma = |\Gamma|\mathrm{e}^{\mathrm{i}\psi_\Gamma}$ and the phase ψ_T of the transmitting coefficient; specifically

$$T = \frac{1}{2}\sqrt{\frac{3}{2}}\sqrt{\frac{\eta_0 k^2}{Y_0\pi}}\sqrt{1-|\Gamma|^2}\;\mathrm{e}^{\mathrm{i}\psi_T} \tag{50}$$

$$R = \sqrt{\frac{3}{2}}\mathrm{i}\sqrt{\frac{\pi Y_0}{\eta_0 k^2}}\sqrt{1-|\Gamma|^2}\;\mathrm{e}^{\mathrm{i}\psi_T} \tag{51}$$

$$S = \frac{3}{4}\mathrm{i}\left(-|\Gamma|\,\mathrm{e}^{\mathrm{i}(2\psi_T - \psi_\Gamma)} + 1\right). \tag{52}$$

The eight scalars needed to specify the magnitudes and phases of T, R, S, and Γ have been reduced by means of the reciprocity and power relations to three scalars (the magnitude and phase of Γ and the phase of T). If the reference plane A_0 in the waveguide feeding the antenna is shifted by a distance ℓ, the phases of T and Γ shift by $\beta_0\ell$ and $2\beta_0\ell$, respectively, where β_0 is the propagation constant of the waveguide mode. Therefore, (52) confirms that the phase of the scattering coefficient S does not change by shifting the waveguide reference plane A_0.

For a lossless scatterer rather than a lossless reciprocal antenna, $T = R = 0$, $|\Gamma| = 1$, and (50)–(52) are replaced by the one lossless power relation in (48) with $T = 0$:

$$|S|^2 = \frac{3}{2}\mathrm{Im}\,(S) \tag{53}$$

or letting $S = |S|\mathrm{e}^{\mathrm{i}\psi}$

$$|S| = \frac{3}{2}\sin\psi \tag{54}$$

a relationship we shall discuss in the next section.

6 INFINITE LINEAR PERIODIC ARRAY OF SMALL PASSIVE ELECTRIC DIPOLE ANTENNAS PERPENDICULAR TO THE ARRAY AXIS

The transmitting, receiving, and scattering coefficients found in Section 5 for a small, reciprocal, lossless z directed electric dipole antenna determine the propagation constants of the

traveling waves that may exist on a linear periodic array of these antennas. To obtain an explicit expression for the dependence of the traveling-wave propagation constant β on the T, R, and S of the antennas composing the array, as well as on the normalized spacing kd of the antennas, consider an infinite linear periodic array of small z directed passive electric dipoles equispaced along the x-axis, each satisfying the scattering-matrix equations (41)–(42)

$$b_0^n = \Gamma a_0^n + R E_z^{0n} \tag{55}$$

$$b_n = T a_0^n + S E_z^{0n} \tag{56}$$

where the subscript n denotes the nth dipole in the infinite array. The dipole antennas are both passive and lossless in that they contain no active or lossy material and each of their feed waveguides are terminated in a perfectly reflecting load with reflection coefficient given by $\Gamma_L = \mathrm{e}^{\mathrm{i}\psi_L}$, such that

$$a_0^n = \Gamma_L b_0^n = \mathrm{e}^{\mathrm{i}\psi_L} b_0^n \tag{57}$$

or

$$b_0^n = \mathrm{e}^{-\mathrm{i}\psi_L} a_0^n \,. \tag{58}$$

Substituting b_0^n from (58) into (55), solving for a_0^n, then using the resulting a_0^n in (56), we find b_n in terms of E_z^{0n}

$$b_n = S_e E_z^{0n} \tag{59}$$

where the "effective" scattering coefficient is defined as

$$S_e = \frac{TR}{\mathrm{e}^{-\mathrm{i}\psi_L} - \Gamma} + S. \tag{60}$$

For a linear array of scatterers rather than antennas, we have $T = R = 0$ and $|\Gamma| = 1$, so that $b_n = S E_z^{on}$ and $S_e = S$. The linear relationship between the amplitude b_n of the nth small z directed dipole and the incident electric field E_z^{on} at the nth dipole is similar to the linear relationship between the amplitude of the electric dipole moment and the incident electric field used in the discrete-dipole approximation for computing scattering by dielectric particles [23], [24]. In this previous discrete-particle scattering work, a full scattering-matrix description was not formulated and neither reciprocity nor power conservation was explicitly applied to reduce the number of variables and required computations.

The field E_z^{0n} is the electric field incident upon the nth small dipole from all the other dipoles. For an infinite array of small z directed electric dipole antennas equally spaced a distance d along the x axis, this incident field E_z^{0n} can therefore be expressed as a summation of the outgoing fields of all but the nth dipole antenna (see (40))

$$E_z^{0n} = \sum_{\substack{j=-\infty \\ j\neq n}}^{+\infty} b_j \frac{\mathrm{e}^{\mathrm{i}kd|j-n|}}{kd|j-n|}\left[1 + \frac{\mathrm{i}}{kd|j-n|} + \frac{1}{(kd)^2|j-n|^2}\right], \quad n = 0, \pm 1, \pm 2, \ldots \pm\infty. \tag{61}$$

Inserting E_z^{0n} from (61) into (59) produces an infinite set of linear equations for the unknown outgoing modal coefficients

$$b_n = S_e \sum_{\substack{j=-\infty \\ j\neq n}}^{+\infty} b_j \frac{\mathrm{e}^{\mathrm{i}kd|j-n|}}{kd|j-n|}\left[1 + \frac{\mathrm{i}}{kd|j-n|} + \frac{1}{(kd)^2|j-n|^2}\right], \quad n = 0, \pm 1, \pm 2, \ldots \pm\infty. \tag{62}$$

The effective scattering coefficient S_e defined in (60) has some remarkable properties. It is the one parameter in (62), besides the normalized separation distance kd, that determines the characteristics of the fields on the linear infinite periodic array of small electric dipoles. Moreover, if the electric dipoles composing the array are reciprocal and lossless, the T, R, and S in the equations (50)–(52) can be inserted into (60) to show that the magnitude and phase of $S_e = |S_e|e^{i\psi_e}$ obey the simple relationship

$$|S_e| = \frac{3}{2}\sin\psi_e. \tag{63}$$

Consequently, ψ_e and kd are the only two independent scalar parameters in the equations (62) that determine the characteristics of the fields supported by the infinite linear periodic array of small z directed electric dipole antennas. Because (63) demands that $\sin\psi_e \geq 0$, the range of ψ_e is limited to

$$0 \leq \psi_e \leq \pi. \tag{64}$$

We also note that the magnitude and phase of S_e are not changed by shifting the reference plane A_0 in the feed waveguide. This result is proven directly from (60) using the facts that the phases of Γ and Γ_L^* shift by $2\beta_0\ell$, the phases of T and R shift by $\beta_0\ell$, and the phase of S remains unchanged (as explained in Section 5) when the reference plane A_0 is shifted by a distance ℓ. (β_0 is the propagation constant of the waveguide mode.)

We shall now use (62) to determine an equation for the traveling-wave propagation constant β as a function of kd and ψ_e. In so doing, we shall also prove that the relationship (63) is not only a consequence of reciprocity and losslessness, but it is a relationship that must be satisfied by the array elements if the array supports a traveling wave. If the array supports a traveling wave with real positive propagation constant β, the b_j in (62) are identical except for a phase shift given by

$$b_j = b_0 e^{i\beta jd} \tag{65}$$

which allows (62) to be rewritten in the form

$$(kd)^3 = S_e \sum_{\substack{j=-\infty \\ j\neq n}}^{+\infty} e^{i\beta d(j-n)} \frac{e^{ikd|j-n|}}{|j-n|}\left[(kd)^2 + \frac{kdi}{|j-n|} - \frac{1}{|j-n|^2}\right], \quad n = 0, \pm 1, \pm 2, \ldots \pm\infty. \tag{66}$$

Each equation in (66) for each different n is identical because the integer index j in the summation ranges from $-\infty$ to $+\infty$. Therefore, simplify (66) by setting $n = 0$ to get

$$(kd)^3 = S_e \sum_{j=1}^{\infty}\left[\frac{e^{i(k+\beta)dj}}{j} + \frac{e^{i(k-\beta)dj}}{j}\right]\left[(kd)^2 + \frac{kdi}{j} - \frac{1}{j^2}\right]. \tag{67}$$

Using the summation formulas [25, sec. 1.441, eqs. 1 and 2; sec. 1.443, eqs. 3 and 5]

$$\sum_{j=1}^{\infty}\frac{\cos na}{n} = \frac{1}{2}\ln\frac{1}{2(1-\cos a)} = -\ln\left[2\sin(a/2)\right], \quad 0 < a < 2\pi \tag{68a}$$

$$\sum_{j=1}^{\infty}\frac{\sin na}{n} = \frac{\pi - a}{2}, \quad 0 < a < 2\pi \tag{68b}$$

$$\sum_{j=1}^{\infty} \frac{\cos na}{n^2} = \frac{\pi^2}{6} - \frac{\pi a}{2} + \frac{a^2}{4}, \quad 0 < a < 2\pi \tag{68c}$$

$$\sum_{j=1}^{\infty} \frac{\sin na}{n^3} = \frac{\pi^2 a}{6} - \frac{\pi a^2}{4} + \frac{a^3}{12}, \quad 0 < a < 2\pi \tag{68d}$$

and the approximations (see Appendix C)

$$\sum_{j=1}^{\infty} \frac{\sin na}{n^2} \equiv F(a) \approx -0.1381 \sin a + 0.03212 \sin 2a - 0.9653a \ln(a/\pi), \quad 0 < a < \pi \tag{69a}$$

$$F(a) = -F(2\pi - a), \quad \pi \leq a < 2\pi \tag{69b}$$

and

$$\sum_{j=1}^{\infty} \frac{\cos na}{n^3} \equiv G(a) \approx 1.3328 - 0.1424 \cos a + 0.01094 \cos 2a + 0.4902a^2 \ln(a/\pi) - 0.2417a^2,$$

$$0 < a < \pi \tag{69c}$$

$$G(a) = G(2\pi - a), \quad \pi \leq a < 2\pi \tag{69d}$$

(67) is reduced to

$$(kd)^3/S_e = -(kd)^2 \ln[2(\cos kd - \cos \beta d)] - kd\,[F(kd + \beta d) - F(\beta d - kd)] -$$

$$[G(kd + \beta d) + G(\beta d - kd)] - \mathrm{i}\frac{2}{3}(kd)^3, \quad kd < \beta d. \tag{70}$$

Writing S_e as $|S_e|e^{i\psi_e}$, equating the real and imaginary parts of (70), and dividing the two resulting equations, one obtains

$$|S_e| = \frac{3}{2} \sin \psi_e, \quad kd < \beta d \tag{71}$$

and

$$\frac{2}{3}(kd)^3 \cos \psi_e + \Big\{(-(kd)^2 \ln\,[2(\cos kd - \cos \beta d)] - (kd)\,[F(kd + \beta d) - F(\beta d - kd)]$$

$$- [G(kd + \beta d) + G(\beta d - kd)]\Big\} \sin \psi_e = 0, \quad kd < \beta d. \tag{72}$$

We emphasize that the equation (71), which was previously derived as (63) using the reciprocity and lossless power conservation relations, has been derived without explicit reference to reciprocity or losslessness. It emerged simply, and rather unexpectedly, as a necessary condition for the array equations (62) to have a traveling-wave solution. For lossless scatterers rather than lossless reciprocal antennas, $S_e = S$ and (71) becomes identical to (54), which was found previously from the power relation for lossless scatterers.

The equation (72) gives an implicit expression for the propagation constant β of the traveling wave supported by the linear periodic array of lossless, passive, electrically small dipoles as a function of the normalized spacing kd of the z directed short dipole antennas and the phase ψ_e of the effective scattering coefficient. Although a closed-form expression

cannot be found for βd as a function of kd and ψ_e as was possible for a linear periodic array of lossless, passive, acoustically small isotropic antennas [13], the implicit expression (72) can be solved numerically for βd given kd and ψ_e. Curves of βd vs kd are plotted in Figure 3 for different values of ψ_e ranging from 10° to 170°; see (64). All the curves have one branch that begins at βd equal to approximately 1.44, the value for which $G(\beta d) = 0$ so that (72) is satisfied when $kd = 0$. All curves for ψ_e less than about 64° have two branches. For the curves for ψ_e less than about 58° one branch begins by being extremely close to the line $\beta d = kd$. Of note is the possibility of two distinct traveling waves that can exist for the same normalized spacing kd and effective scattering coefficient phase ψ_e. If, for example, we follow the line $kd = 1$ we see that it intersects the branches of the $\psi_e = 45°$ curve in two places corresponding to two distinct values of the traveling wave propagation constant β. The possibility that two distinct traveling waves can be excited is quite different from the behavior encountered when an infinite array of isotropic acoustically small transducers was studied for which only one traveling wave can be excited [13]. By referring to the definition of S_e in (60), we see that the phase ψ_e (and magnitude) of S_e can be adjusted by changing the phase ψ_L of the reflection coefficient of the perfectly reflecting loads that terminate the feed waveguides of the passive dipole elements of the array. This adjustment can be done, in principle, by changing the lengths of the feed waveguides, or by changing the material properties of the terminating loads. However, unless the dipoles are fed through a ground plane, it may be difficult in practice to appreciably vary ψ_e in this way and keep the dipole spacing small enough to maintain a traveling wave. In general, the scattering phase ψ_e of an electric dipole will change with frequency. In that case, the propagation constant β of the traveling wave can be varied without changing ψ_e if the separation distance d of the array elements is varied while holding the frequency fixed.

In a laboratory, measurements of the propagation constant of a traveling wave and its variation with the electrical spacing of the array elements, kd, could be efficiently performed by varying the frequency, keeping the dipole length and dipole separation constant. In this case the ratio of the length of the dipoles to the separation of adjacent dipoles, $2h/d$, would be fixed as would the ratio of the wire radius to the wire length, ρ/h. Examples of the theoretical $kd - \beta d$ curves are illustrated in Figure 4 in which three $kd - \beta d$ curves corresponding to different values of $2h/d$ and with $\rho/(2h) = 0.1$ are shown. The curves begin at the line $\beta d = kd$ and end when $\beta d = \pi$. A unique value of the traveling wave propagation constant β is associated with a given value of kd. The group velocity $\mathrm{d}k/\mathrm{d}\beta$ is positive for all three curves. These calculations require values of the phase, ψ_e, of the effective scattering coefficient as a function of h/λ for fixed ρ/h. These values can be obtained using standard scattering codes such as NEC [26] and CICERO [27] since if a thin short wire is illuminated by a plane wave with the electric field parallel to the wire, the scattered far field is given by (see (40)) $E_z^{sc} = be^{ikr}/(kr)$ with (see (59)) $b = S_e E_z^0$ so that S_e is the ratio of the scattered field to the incident field.

The theoretical calculations of the propagation constant β of the traveling wave based on (72) can be verified in part by reference to measurements made by Ehrenspeck and Poehler [1] who measured the phase velocity on a Yagi array as a function of the height of the directors for two different spacings and two different wire radii. The $kd - \beta d$ diagram given in Figure 3 plots βd as a function of kd and ψ_e, the phase of the effective scattering coefficient $S_e = \frac{3}{2}\sin\psi_e e^{i\psi_e}$. Since the phase velocity is equal to $kd/\beta d$, to compare our theoretical

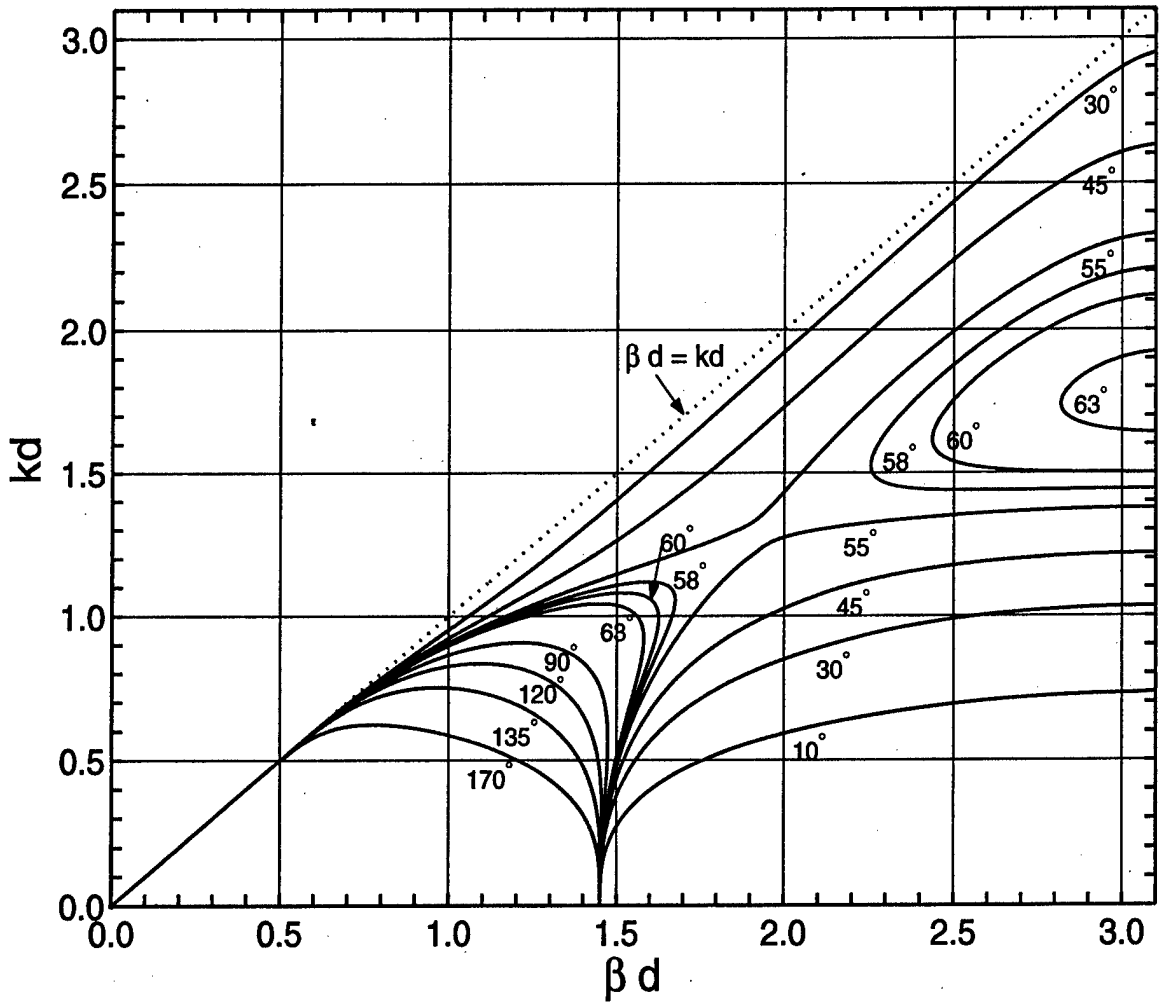

Figure 3: kd–βd curves for an infinite linear periodic array of short parallel electric dipoles perpendicular to the array axis with different values of the phase ψ_e of the effective scattering coefficient.

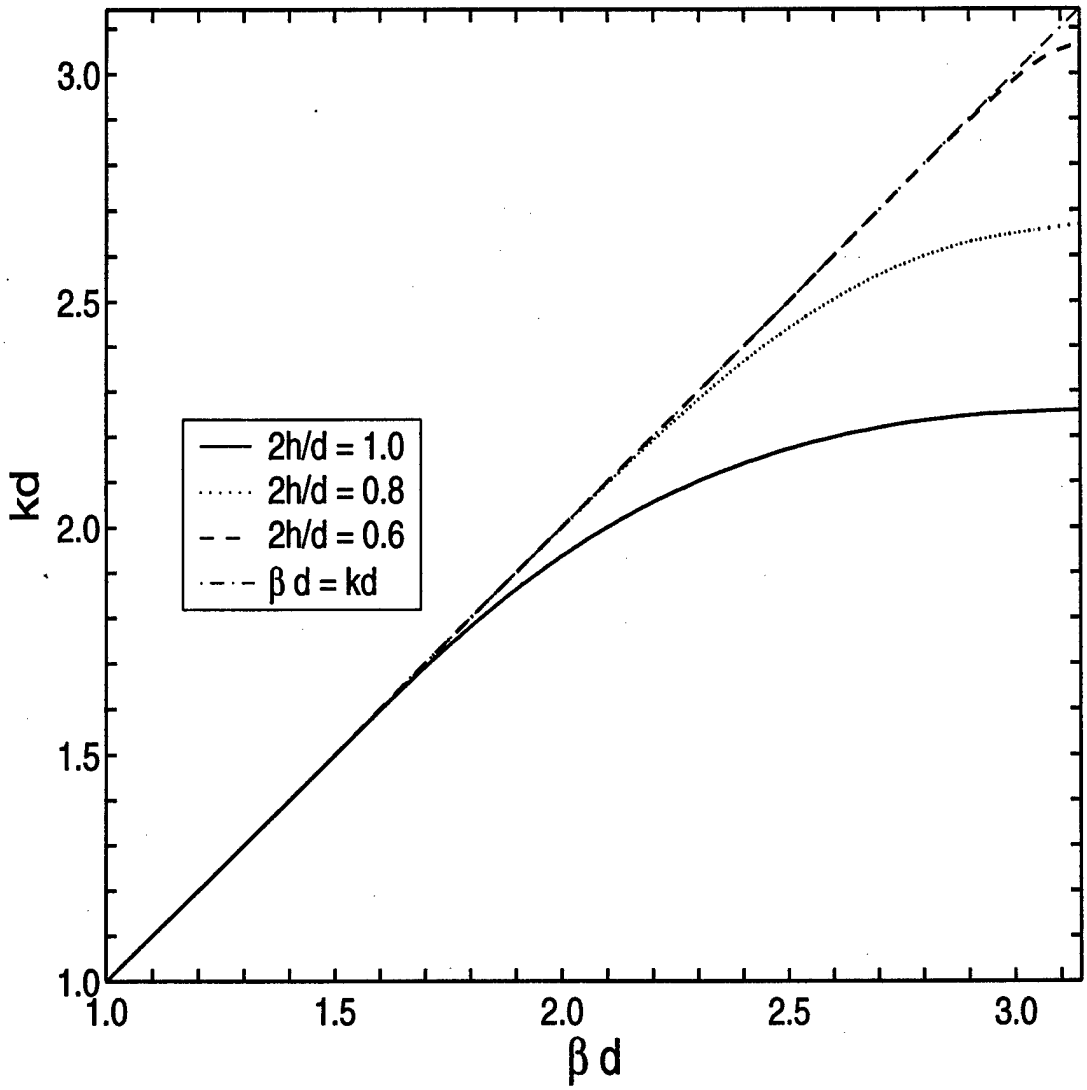

Figure 4: kd–βd curves for an infinite linear periodic array of short parallel electric dipoles perpendicular to the array axis with different ratios of the dipole length to the dipole separation ($2h/d$). The ratio of the radius of the dipole to its length is given by $\rho/(2h) = 0.1$.

results with the experimental results of Ehrenspeck and Poehler we need to obtain ψ_e for thin short wires of different heights and radii. This was done using NEC. In Figure 5 we show plots of ψ_e versus wire half-length h/λ for short thin wires of three different radii. Figure 6 shows curves of the theoretical phase velocity of the traveling wave on an infinite array of wires with spacing $d/\lambda = 0.2$ and radii $\rho/\lambda = 0.012$ and 0.024 as a function of the wire half-length h/λ along with experimental values taken from Figure 13 of [1]. Figure 7 shows the corresponding curves for a spacing of $d/\lambda = 0.4$. Considering the difficulty of making the measurements the agreement is quite good, especially for the shorter wires. As the length of the wires increases the assumption that the fields of the wires are those of elementary electric dipoles becomes increasingly inaccurate.

7 FINITE LINEAR PERIODIC ARRAY OF SMALL ELECTRIC DIPOLES PERPENDICULAR TO THE ARRAY AXIS

The traveling-wave propagation constant given implicitly by (72) was found by solving analytically the coupled scattering-matrix equations for an infinite linear periodic array of small z directed electric dipoles equispaced along the x axis. We used an infinite rather than a finite number of identical array elements to derive (72) because only on an infinite array can a traveling wave exist alone as an exact homogeneous solution. For a linear periodic array with a finite number of these same antenna elements, the same traveling wave can exist, but it is always accompanied by the portion of the excitation fields that do not couple to the traveling wave and by the fields generated through diffraction from both ends of the finite array. In this section we consider such an array of N identical small z directed electric dipole elements separated along the x axis by a distance d, as shown in Figure 8. All the antenna elements of this linear array except the first one are terminated in a perfectly reflecting load with reflection coefficient given by $\Gamma_L = e^{i\psi_L}$. The first antenna in the array is fed by an incident waveguide modal coefficient a_0^1.

We can use the scattering-matrix equations (55)–(56) to derive a set of N linear equations for the N unknown outgoing wave coefficients b_n for each of the array elements ($n = 1, 2, 3, \ldots N$). The derivation leading to the equations in (62) for the passive electric dipole elements in the infinite array applies also to the passive z directed electric dipole elements ($n = 2, 3, \ldots N$) of the finite array. Thus, we can immediately write down $N - 1$ of the required equations for the finite array as

$$b_n - S_e \sum_{\substack{j=1 \\ j \neq n}}^{N} b_j \frac{e^{ikd|j-n|}}{kd|j-n|} \left[1 + \frac{i}{kd|j-n|} - \frac{1}{(kd)^2|j-n|^2} \right] = 0, \quad n = 2, 3, \ldots N. \tag{73}$$

The feed-element equation ($n = 1$) can be found by inserting E_z^{01} from (61) into (56) to get

$$b_1 - S \sum_{j=2}^{N} b_j \frac{e^{ikd|j-1|}}{kd|j-1|} \left[1 + \frac{i}{kd|j-1|} - \frac{1)}{(kd)^2|j-1|^2} \right] = T a_0^1. \tag{74}$$

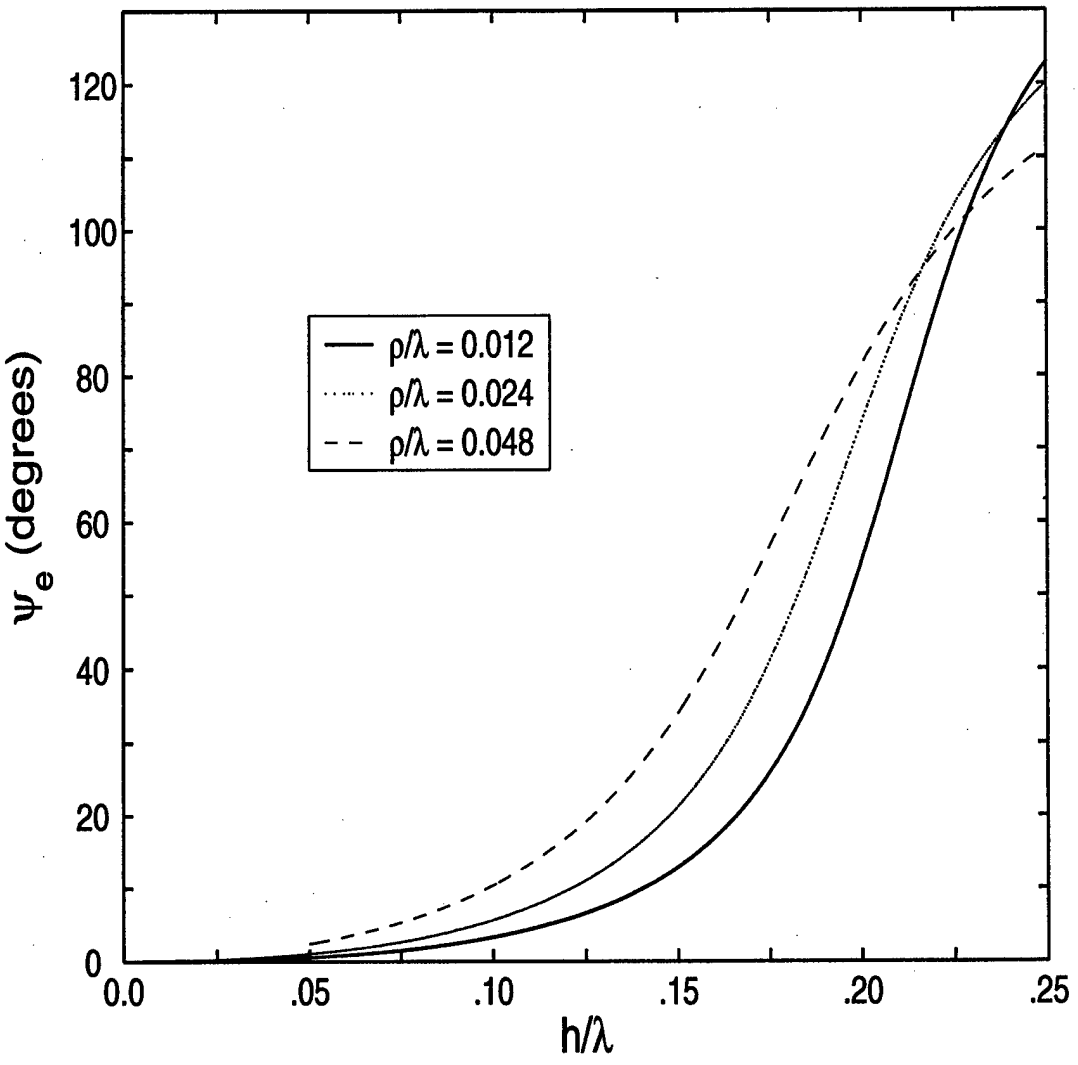

Figure 5: Phase ψ_e of the effective scattering coefficient of a thin perfectly conducting wire as a function of the wire half-length h/λ.

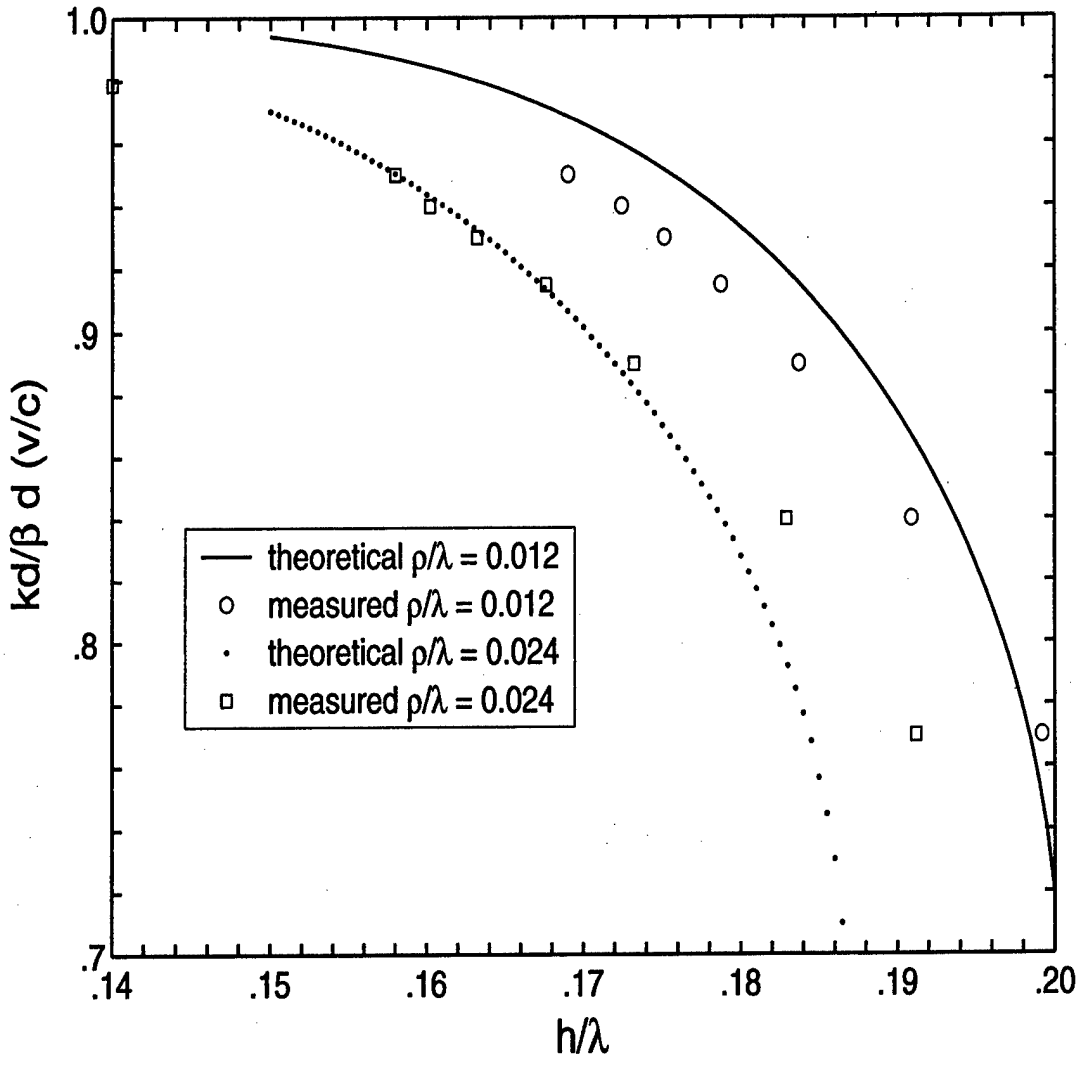

Figure 6: Theoretical curves of the relative phase velocity of a traveling wave on an infinite linear periodic array of thin wires perpendicular to the array axis with radii $\rho/\lambda = 0.012$ and 0.014 as a function of the wire half-length h/λ compared with experimentally determined values of the relative phase velocity of a traveling wave on a long Yagi antenna; spacing $d/\lambda = 0.2$.

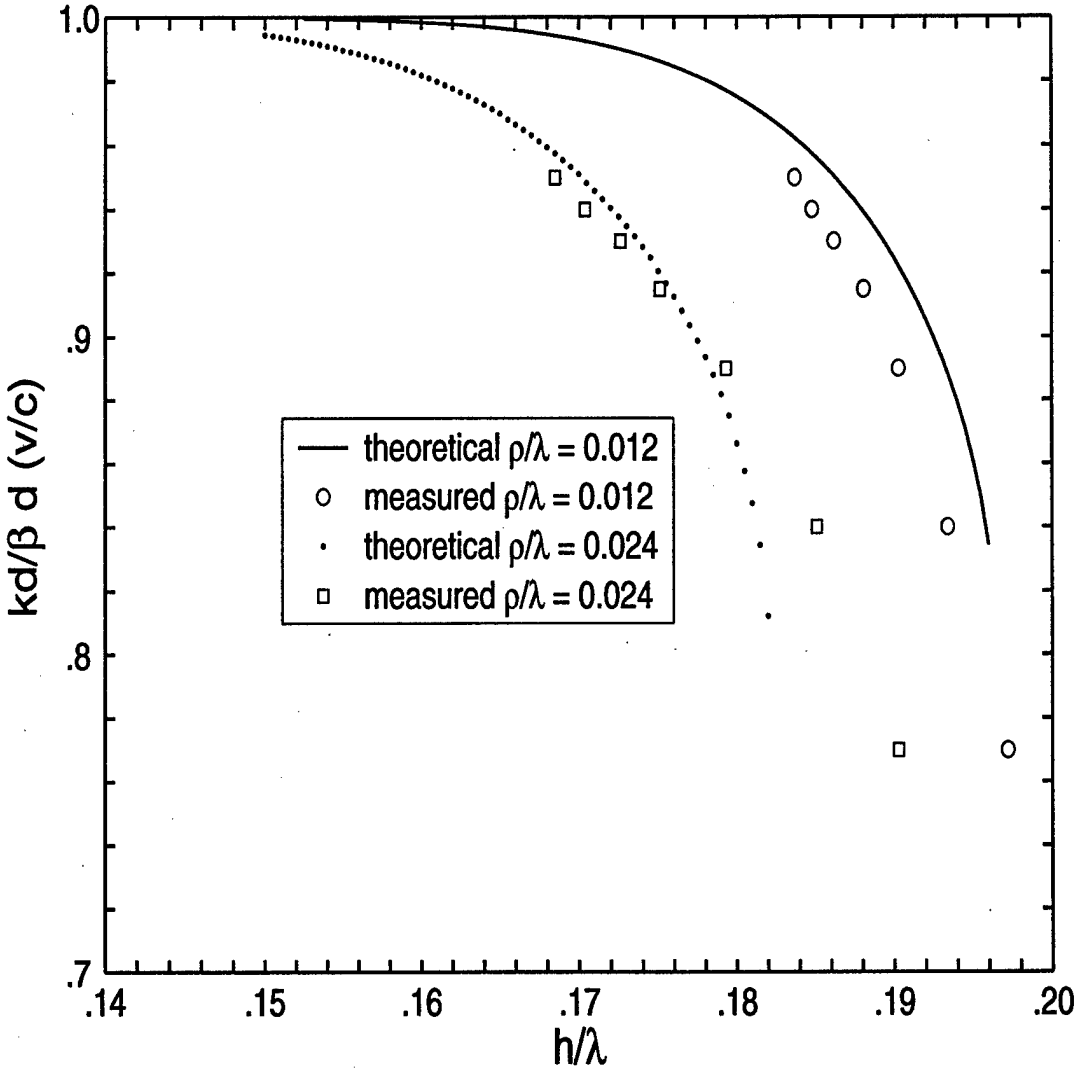

Figure 7: Theoretical curves of the relative phase velocity of a traveling wave on an infinite linear periodic array of thin wires perpendicular to the array axis with radii $\rho/\lambda = 0.012$ and 0.014 as a function of the wire half-length h/λ compared with experimentally determined values of the relative phase velocity of a traveling wave on a long Yagi antenna; spacing $d/\lambda = 0.4$.

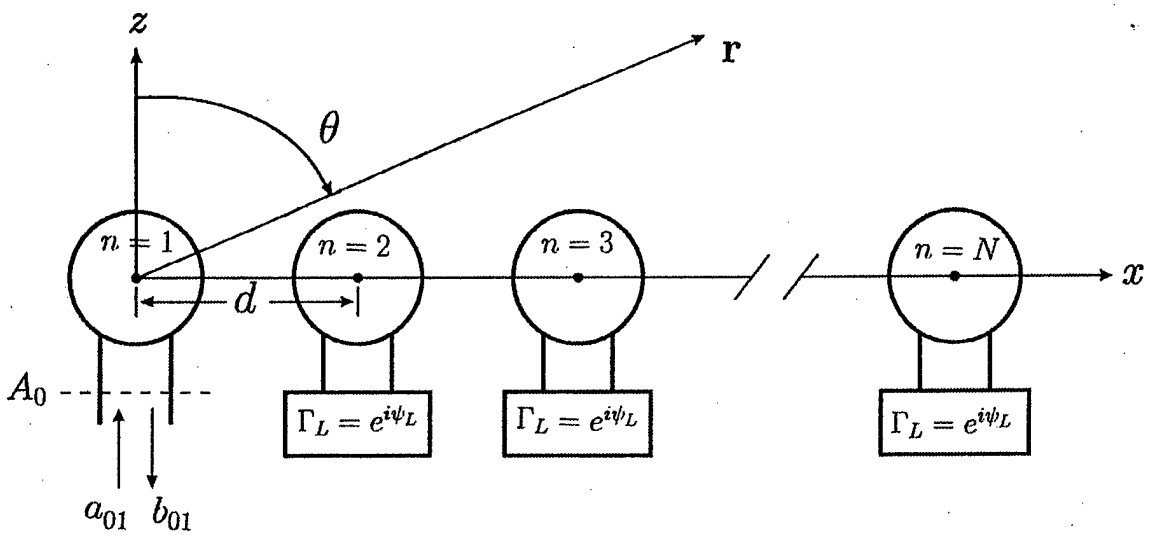

Figure 8: Finite linear periodic array of N short electric dipole antennas (represented by the circles) perpendicular to the array axis separated by a distance d along the x axis. The waveguides of all the elements of the array are terminated in the perfectly reflecting passive load $\Gamma_L = e^{i\psi_L}$ except the first element, which is fed with an incident waveguide modal coefficient a_0^1.

The solution to the set of N linear equations in (73)–(74) is a trivial matter on a computer. It is helpful, however, to specify the scattering-matrix parameters in these equations in a convenient form. First, we note that it is unnecessary to specify the transmitting coefficient T on the right hand side of (74) because it is multiplied by the one excitation coefficient a_0^1, which can be chosen arbitrarily. Therefore, for the sake of simplicity, let

$$Ta_0^1 = 1 \tag{75}$$

in (74). Secondly, since S_e satisfies (63) and (71), express S_e in (73) as

$$S_e = \frac{3}{2}\sin\psi_e e^{i\psi_e}, \qquad 0 \le \psi_e \le \pi. \tag{76}$$

Thirdly, use (52) to rewrite S in (74) as

$$S = \frac{3}{2}|\Gamma|\sin\alpha e^{i\alpha} + \frac{3}{4}i(1-|\Gamma|), \qquad 0 \le \alpha \le \pi, \quad 0 \le \Gamma \le 1, \tag{77}$$

where

$$\alpha = \tan^{-1}\frac{1-\cos(2\psi_T - \psi_\Gamma)}{\sin(2\psi_T - \psi_\Gamma)}. \tag{78}$$

Consequently, there are four scalar parameters (kd, ψ_e, α and $|\Gamma|$), in addition to the number of elements N in the array, that must be chosen to get a numerical solution to (73)–(74). We found, however, that the numerical solution to (73)–(74) did not change qualitatively as α and $|\Gamma|$ were varied over their full range of values. In other words, S in (74), unlike S_e in (73), is not a critical parameter that must be varied if one merely wants to display different representative numerical solutions. In the numerical results shown below, the values of α and $|\Gamma|$ were set equal to 90° and .5, respectively, so that S has the value of

$$S = 1.125i\,. \tag{79}$$

We also found that the solution to a multi-element array does not change qualitatively with the number of elements.[2] The numerical results shown below that do not depend qualitatively on varying N are computed for the representative value of $N = 40$. This leaves us with just two critical parameters, kd and ψ_e, to specify when solving for the b_n in equations (73)–(74).

Once the b_n are computed from (73)–(74), the electromagnetic field radiated by the array can be computed from the formulas

$$\mathbf{E}(\mathbf{r}) =^{r\to\infty}_{\sim} \frac{e^{ikr}}{kr}\sum_{n=1}^{N} b_n e^{-ikd(n-1)\sin\theta\cos\phi}\sin\theta\,\hat{\boldsymbol{\theta}} \tag{80a}$$

$$\mathbf{H}(\mathbf{r}) =^{r\to\infty}_{\sim} Y_0\hat{\mathbf{r}}\times\mathbf{E}(\mathbf{r}) \tag{80b}$$

[2]For example, the number of resonant peaks in Figure 9 would change in approximate proportion to the number of elements N, but the height (≈ 1.3) of the resonant peaks and their cut-off at $kd \approx 2.5$ would remain about the same.

where θ is the spherical angle that the vector $\mathbf{r}$ to the far field makes with the z axis. The total power radiated by the array, and the directivity function for the array are given in terms of the electric far field by

$$P = \frac{Y_0}{2} \int_0^{\pi} \int_0^{2\pi} |r\mathbf{E}(\mathbf{r})|^2_{r\to\infty} \sin\theta d\phi d\theta \tag{81}$$

and

$$D(\mathbf{r}) = \lim_{r\to\infty} \frac{4\pi |r\mathbf{E}(\mathbf{r})|^2}{\int_0^{\pi} \int_0^{2\pi} |rE(\mathbf{r})|^2 \sin\theta \mathrm{d}\phi \mathrm{d}\theta} . \tag{82}$$

If only the feed electric dipole element ($n = 1$) were present in free space, it would radiate a power equal to the net power it received from the waveguide, namely

$$P_0 = \frac{1}{2}\eta_0 |a_0^1|^2 (1 - |\Gamma|^2) \tag{83}$$

or in view of (75) and (45)

$$P_0 = \frac{4\pi Y_0}{3k^2} . \tag{84}$$

The power ratio

$$\mathcal{R} \equiv \frac{P}{P_0} = \frac{3k^2}{8\pi} \int_0^{\pi} \int_0^{2\pi} |r\mathbf{E}(\mathbf{r})|^2_{r\to\infty} \sin\theta \mathrm{d}\phi \mathrm{d}\theta \tag{85}$$

is greater than or less than 1 depending on whether the array radiates more or less power than the feed element radiates alone in free space. We can also express $\mathcal{R}$ in terms of the magnitude of the in situ waveguide-mode reflection coefficient Γ_1 looking into the feed electric dipole.

$$\mathcal{R} = \frac{1 - |\Gamma_1|^2}{1 - |\Gamma|^2} . \tag{86}$$

where $b_0^1 = \Gamma_1 a_0^1$ and the total power radiated can also be expressed as $P = \frac{1}{2}\eta_0 |a_0^1|^2 (1 - |\Gamma_1|^2)$, the power accepted by the feed element, because the array is lossless. If $\mathcal{R}$ becomes much less than 1, the voltage required to feed a fixed amount of power into the array will grow much greater than that required to feed the same power into the feed element when it resides alone. In other words, $\mathcal{R} \ll 1$ means that the magnitude of the in situ waveguide-mode reflection coefficient $|\Gamma_1|$ looking into the feed electric dipole ($n = 1$) is significantly closer to unity than its reflection coefficient $|\Gamma|$ when all the other dipoles ($n = 2, 3, \ldots N$) are removed.

From (81), (82) and (85) together with (80a) the directivity and power ratio for the finite linear array along the x-axis of short z directed dipoles can be calculated respectively from

$$D(\theta, \phi) = \frac{\left| \sum_{n=1}^{N} b_n \mathrm{e}^{-\mathrm{i}kdn \sin\theta \cos\phi} \right|^2 \sin^2\theta}{2\Delta} \tag{87}$$

and

$$\mathcal{R} = 3\Delta \tag{88}$$

where

$$\Delta = \frac{1}{3}\sum_{n=1}^{N}|b_n|^2 + \frac{1}{2}\sum_{n=1}^{N-1}\sum_{m=n+1}^{N}\mathrm{Re}[b_n b_m^*]\int_0^{\pi} J_0[(m-n)kd\sin\theta]\sin^3\theta \mathrm{d}\theta \tag{89}$$

and we have made use of the integration formula $\int_0^{2\pi}\exp(iu\cos\phi)\mathrm{d}\phi = 2\pi J_0(u)$ with J_0 the Bessel function of zero order. The $N(N-1)$ numerical integrations required to calculate the directivity and power ratio can be avoided if instead of the cartesian xyz coordinate system we have been using with the x axis along the array axis and the z axis parallel to the electric dipoles we switch to a cartesian $x'y'z'$ system with the z' axis along the array axis and the x' axis parallel to the electric dipoles (i.e., $\hat{\mathbf{z}}' = \hat{\mathbf{x}}, \hat{\mathbf{x}}' = \hat{\mathbf{z}}, \hat{\mathbf{y}}' = -\hat{\mathbf{y}}$). The directivity and power ratio can then be obtained in closed form:

$$D(\theta',\phi') = \frac{\left|\sum_{n=1}^{N} b_n \mathrm{e}^{-ikdn\cos\theta'}\right|^2 (1-\sin^2\theta'\cos^2\phi')}{2\Delta} \tag{90}$$

and

$$\mathcal{R} = 3\Delta \tag{91}$$

where

$$\Delta = \frac{1}{3}\sum_{n=1}^{N}|b_n|^2 + \sum_{n=1}^{N-1}\sum_{m=n+1}^{N}\mathrm{Re}[b_n b_m *]\left(\mathrm{sinc}[(m-n)kd]\left[1-\frac{1}{[(m-n)kd]^2}\right] + \frac{\cos[(m-n)kd]}{[(m-n)kd]^2}\right). \tag{92}$$

7.1 NUMERICAL RESULTS FOR THE FINITE ARRAY

The power ratio $\mathcal{R}$ defined in (85) is plotted as a function of kd in Figures 9 and 10 for a 40 element linear array of small z directed electric dipoles equispaced along the x-axis. In Figure 9 the phase ψ_e of the effective scattering coefficient has been chosen equal to 45° and in Figure 10 it equals 135°. In Figure 9 we note that the curve has a region of large oscillations followed by a region of small more equally spaced oscillations and ending with a non-oscillatory portion. This seemingly curious behavior can be understood qualitatively with reference to the $kd - \beta d$ diagram of Figure 3. For values of kd between 0.4 and about 1.2 two distinct traveling waves can be excited, one with a phase constant close to that of free space, and the other increasing from βd equal to about 1.44 to π. Apparently the two traveling waves can both highly constructively and destructively interfere with each other resulting in large oscillations of the power ratio. Also note that one of the traveling wave propagation constants is much larger than k. The impedance mismatch of this traveling wave as it encounters free space at the ends of the array will be large, and an appreciable amount of power will be reflected so that a large standing wave can be supported by the array. For kd between 1.2 and a little more than 2.6 only one traveling wave can be excited. The propagation constant of this traveling wave is fairly close to k so that the impedance mismatch of this wave as it encounters free space at the array ends is not very pronounced with the result that the corresponding standing wave has a relatively small amplitude. For

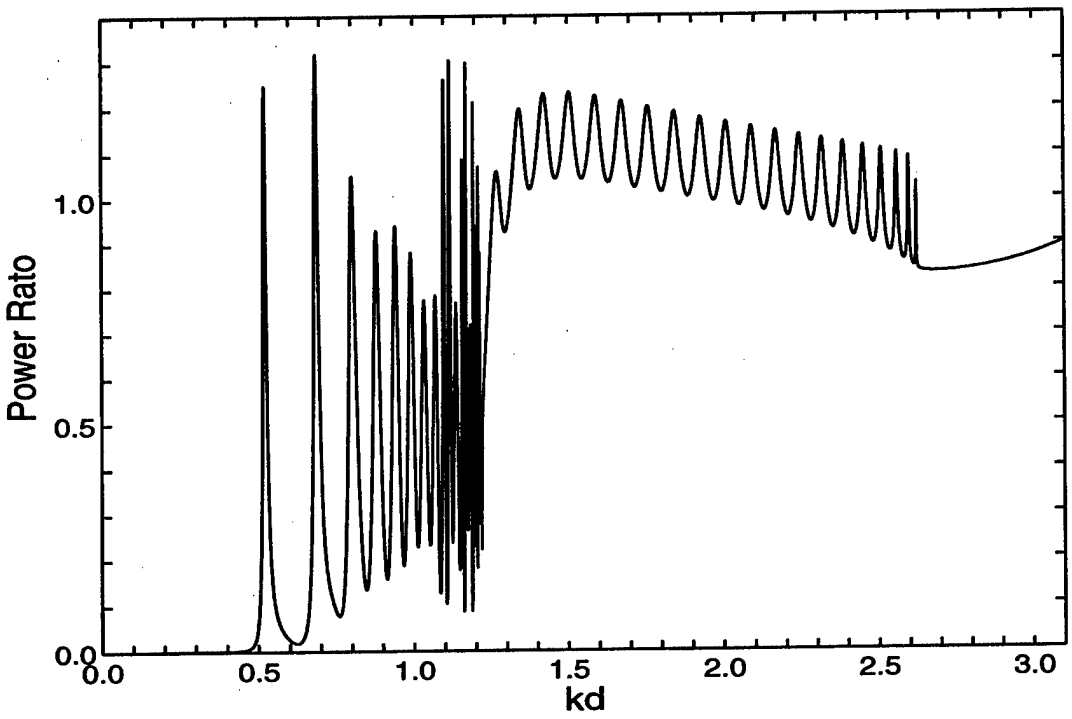

Figure 9: Power ratio versus kd for a forty element linear periodic array of short electric dipoles perpendicular to the array axis $\psi_e = 45°$.

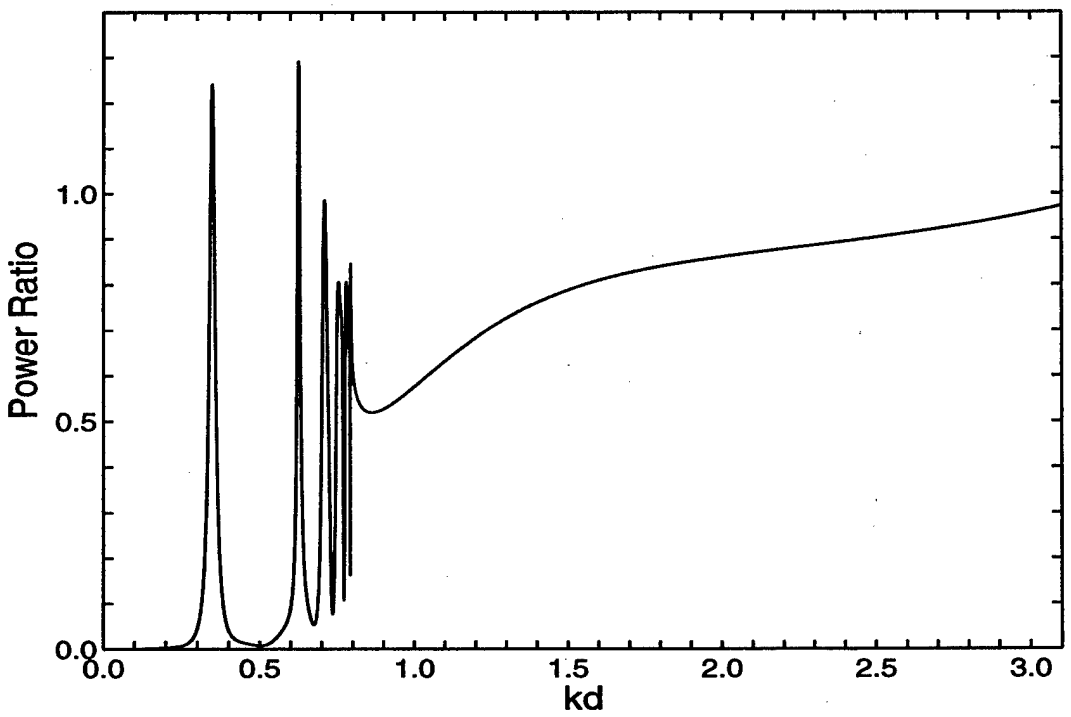

Figure 10: Power ratio versus kd for a forty element linear periodic array of short electric dipoles perpendicular to the array axis with $\psi_e = 135°$.

kd larger than about 2.6 no traveling wave can be excited and so there are no oscillations of the power ratio. The array radiates more or less like the feed element only in free space because none of the feed element radiation excites a traveling wave. The scattering excitation of the passive elements decreases rapidly with increasing distance from the feed element.

In Figure 10 the power ratio is plotted as a function of kd for $\psi_e = 135°$. Again the $kd - \beta d$ diagram of Figure 3 can be used to understand the behavior of the curve. For kd less than about 0.7, although in principle two traveling waves can exist, one has a propagation phase constant almost exactly equal to that of free space and cannot be excited with a small feed element. For kd between about 0.7 and 0.8 two traveling wave can be excited resulting in the more rapid oscillations of the power ratio. Finally for still larger values of kd no traveling wave can be excited and the power ratio slowly approaches the value of 1 for larger interelement spacing.

An interesting feature of Figures 9 and 10 is that the resonant peaks in the power ratio never get higher than a value of about 1.3. Therefore, the magnitude of the in situ waveguide-mode reflection coefficient $|\Gamma_1|$ given in (86) never gets much less than the magnitude of the reflection coefficient $|\Gamma|$ of the feed element radiating alone in free space. At kd values between pronounced resonant peaks, however, the power ratio becomes much less than unity, $|\Gamma_1|$ gets much closer to unity than $|\Gamma|$, and it takes a much higher voltage to feed the array with the same amount of accepted power as the power accepted at the resonant peaks or when the feed antenna is radiating alone in free space. Although the curves in Figures 9 and 10 were computed for $|\Gamma| = .5$, the resonant peaks in the power ratio do not exceed a value of about 2 as $|\Gamma| \to 1$. Thus, operating at a resonant peak of the array does not eliminate the difficulty of feeding appreciable power into small electric dipoles. To enable more power to be accepted and radiated by an array of small elements, Veremey and Mittra [10] have designed each small element to be a resonant antenna with a reasonably low reflection coefficient. This elemental resonance is superposed on the curves corresponding to those in Figures 9 and 10 for their arrays. When the elemental resonance occurs near an array resonance, the array resonance appears to "split" into two resonances.

Figure 11 shows two far-field directivity patterns computed from (82) for the 40 element array, one with $kd = 2.1$ and $\psi_e = 30°$ and the other for $kd = 1.9$ and $\psi_e = 63°$. Since the $kd = 2.1$ array is a little longer than the $kd = 1.9$ array it is to be expected that the directivity will oscillate more rapidly for the larger array than for the smaller one. Also, referring to the $kd - \beta d$ diagram of Figure 3 again, we see that the traveling wave propagation constant for the array with $kd = 2.1$ and $\psi_e = 30°$ is quite close to k and so the associated phase velocity is close to the speed of light. In contrast, the phase constant for the array with $kd = 1.9$ and $\psi_e = 63°$ is considerably larger than k and so the associated phase velocity is considerably less than the speed of light. The larger endfire directivity obtained for the array with the larger phase velocity is an example of a general trend predicted many years ago by Hansen and Woodyard [14].

The difference in endfire directivities seen in Figure 11 can be made much less by changing the number of elements N for the $\psi_e = 63°$ array to a value for which the traveling wave launched from the end of the array and the feed radiation that is not converted to the traveling wave add in phase (or nearly in phase) in the far field at $\theta = 0°$. Nonetheless, the maximum endfire directivity attainable by varying the number of elements in the array becomes greater with increasing phase velocity of the traveling wave. We demonstrate this

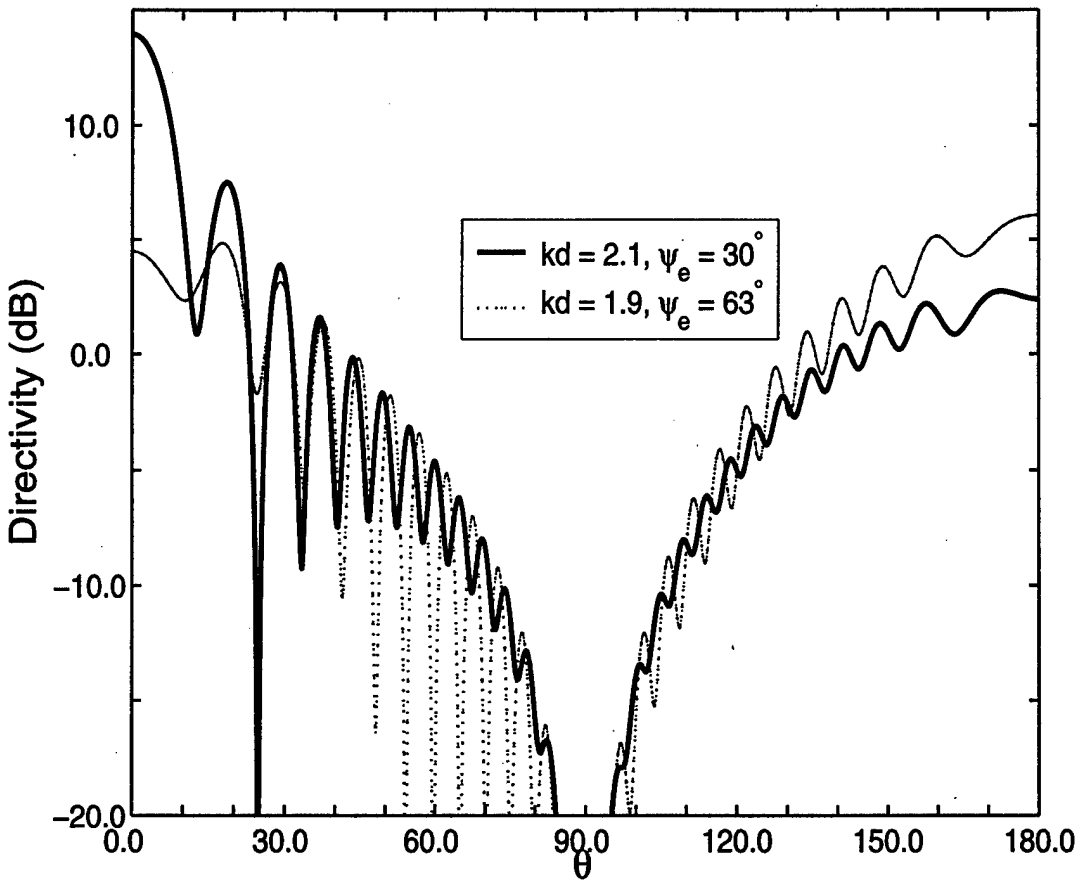

Figure 11: Directivity patterns for a forty element linear periodic array of short electric dipoles perpendicular to the array axis with $kd = 2.1$ and $\psi_e = 30°$, and $kd = 1.9$ and $\psi_e = 63°$.

in Figure 12 in which the maximum directivity in the endfire direction ($\theta = 0°$), obtained by varying N from 2 to 100, is plotted versus the normalized phase velocity of the traveling wave $[v/c = kd/(\beta d)]$ for three different values of kd chosen with reference to Figure 3 so that only one traveling wave can be excited. The general increase of the maximum endfire directivity with increasing relative phase velocity v/c is in agreement with the prediction of Hansen and Woodyard [14] (for closely spaced elements, $d/\lambda < 1/3$, and ignoring reflections of the traveling wave from the ends of the array) and determined experimentally by Ehrenspeck and Poehler [1]. Of course, the maximum attainable endfire directivity of a linear array of N closely spaced isotropic radiators, for which the magnitude and phase of the excitation coefficients of the N elements can be specified arbitrarily, is much larger than the maximum attainable endfire directivity shown in Figure 12 for the array with one feed element [28].

8 LINEAR PERIODIC ARRAYS OF SMALL ELECTRIC DIPOLES PARALLEL TO THE ARRAY AXIS

In Sections 6 and 7 we considered linear periodic arrays of small electric dipole antennas perpendicular to the array axis. In this section we investigate linear periodic arrays of small electric dipole antennas in which the dipoles are aligned with the array axis. We begin by considering the possibility of traveling waves on an infinite array. We consider z directed small electric dipoles and take the z axis as the array axis. The nth electric dipole in the array is excited by the z component only of the fields radiated by all the other dipoles in the array. Similarly to (61), from (35a) and (39) the field in the z direction incident on the nth dipole is given by

$$E_z^{0n} = 2 \sum_{\substack{j=-\infty \\ j\neq n}}^{+\infty} b_j \frac{e^{ikd|j-n|}}{(kd)^2|j-n|^2} \left(-i + \frac{1}{kd|j-n|}\right), \quad n = 0, \pm 1, \pm 2, \ldots \pm \infty. \tag{93}$$

Inserting E_z^{0n} from (93) into (59), assuming the existence of a traveling wave (65), and letting $n = 0$ yields the equation similar to (67)

$$(kd)^3 = 2S_e \sum_{j=1}^{\infty} \left[\frac{e^{i(k+\beta)dj}}{j^2} + \frac{e^{i(k-\beta)dj}}{j^2}\right] \left(-kdi + \frac{1}{j}\right). \tag{94}$$

Using the summation formulas (68c) and (68d) and the approximate summations (69a) and (69c) we obtain similarly to (71) and (72),

$$|S_e| = \frac{3}{2} \sin\psi_e, \quad kd < \beta d \tag{95}$$

and

$$-\frac{1}{3}(kd)^3 \cos\psi_e + \{kd\,[F(kd+\beta d) - F(\beta d - kd)] + [G(kd+\beta d) + G(\beta d - kd)]\} \sin\psi_e = 0, \quad kd < \beta d. \tag{96}$$

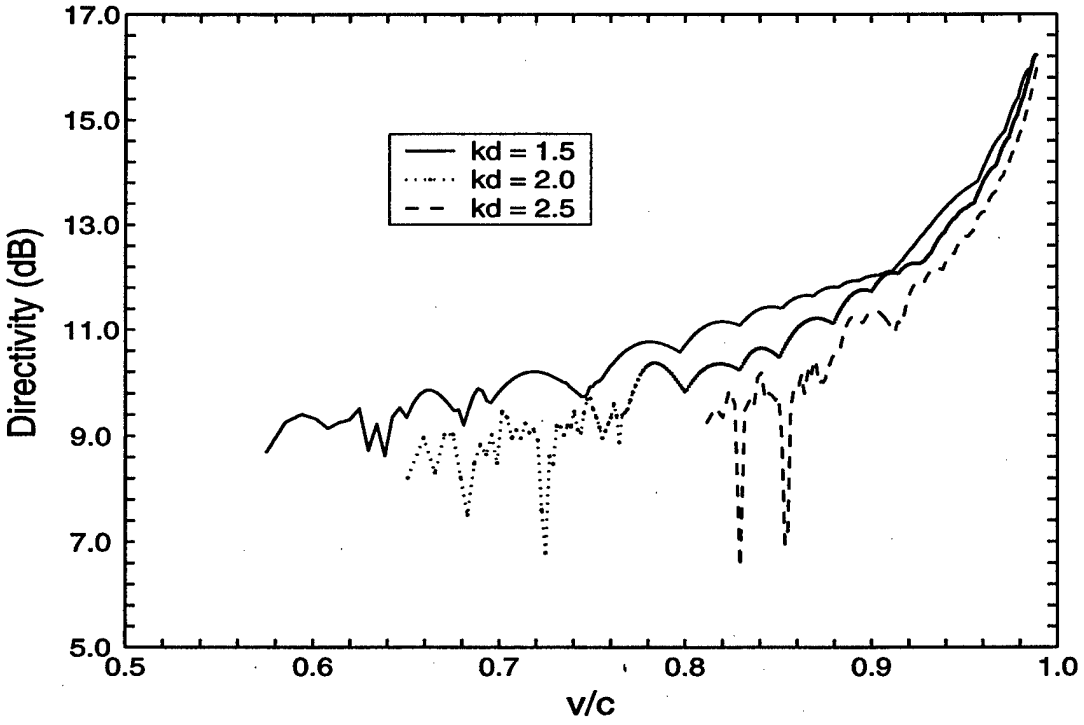

Figure 12: Maximum endfire directivity versus relative phase velocity for a linear periodic array of short electric dipoles perpendicular to the array axis.

The implicit expression (96) can be solved numerically for βd given kd and ψ_e. Curves of βd vs kd are plotted in Figure 13 for different values of ψ_e ranging from 0.1° to 170°; see (64). In contrast with the $k\beta - kd$ diagram of Figure 3 for traveling waves on the infinite array of short electric dipoles perpendicular to the array axis, here there is only one branch of the curve for each value of ψ_e. All the curves begin at βd equal to approximately 1.44, the value for which $G(\beta d) = 0$ so that (96) is satisfied when $kd = 0$. Since a horizontal line for a constant value of kd intersects one of the curves in only one place, at most one traveling wave can be supported by an infinite array of short electric dipoles aligned with the array axis.

Whether in fact it is possible for a traveling wave to be supported on a linear periodic array of thin wire scatterers aligned with the array axis depends on the actual value of ψ_e for the thin short wires of a given length $2h$ and radius ρ that compose the array. We note first that $2h < d$ where d is the separation of the centers of adjacent wires in the array. Additionally the length of the wires should be considerably greater than the wire diameter, say $2h > 4\rho$, for the dipole pattern (37) to hold. Thus the wire length, radius, and separation must satisfy the inequality

$$4k\rho < 2kh < kd. \tag{97}$$

Suppose, for example, that $\rho = 0.024\lambda$. Then $k\rho = 0.15$, $kh > 0.30$, and $h/\lambda > 0.05$. Referring to Figure 5 where we have plotted the phase ψ_e of the effective scattering coefficient versus wire length for wires of different radii we can tabulate $h/\lambda, \psi_e$, and $2kh$ for values of $h/\lambda \geq 0.05$

h/λ	$2kh$	ψ_e
0.05	0.63	1.04°
0.06	0.75	1.58°
0.07	0.88	2.26°
0.08	1.01	3.13o
0.09	1.13	4.25°
0.10	1.26	5.66°

Now from the second inequality of (97) we see by referring to Figure 13 that the minimum value of ψ_e necessary for a traveling wave to be supported by an array of wires of the given half-length h/λ is equal to the value of ψ_e of the $k\beta - kd$ curve that intersects the $k\beta = kd$ line at $k\beta = 2kh$. In all cases it is found that this minimum value of ψ_e is greater than the actual value of ψ_e tabulated for the wires of the given length and radius. Since this same result is found to hold for wires with other values of ρ we conclude that no traveling wave can actually be excited on an array of short thin wires aligned with the array axis (unless the thin wires are loaded to substantially increase the value of ψ_e).

9 LINEAR PERIODIC ARRAYS OF SMALL ELECTRIC DIPOLES SKEW TO THE ARRAY AXIS

In this section we consider linear periodic arrays of small electric dipole antennas in which the dipoles are inclined at an angle θ_0 to the array axis [29] (see Figure 14). The electric

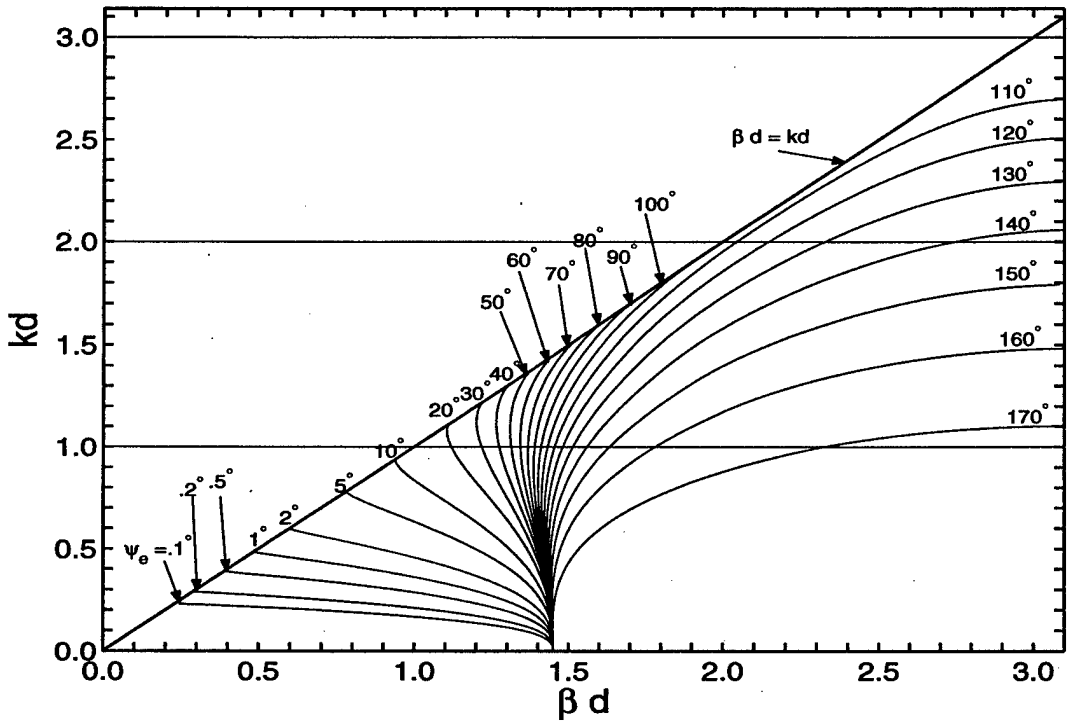

Figure 13: kd–βd curves for an infinite linear periodic array of short electric dipoles aligned with the array axis with different values of the phase ψ_e of the effective scattering coefficient.

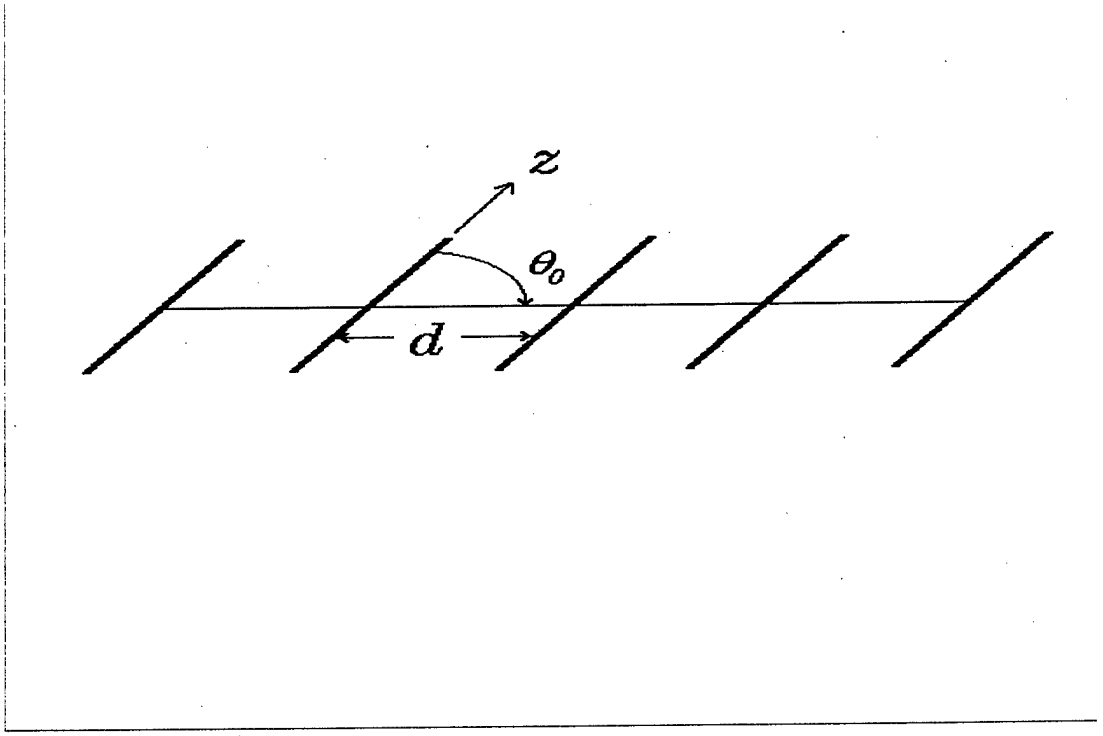

Figure 14: Linear periodic array of short electric dipoles oriented at an angle θ_0 with respect to the array axis.

dipoles are taken to be in the z direction. To investigate the possibility of traveling waves on an infinite array we note that the nth electric dipole in the array is excited by the z component only of the fields radiated by all the other dipoles in the array. Since the z component of the electric field radiated by a short z directed electric dipole is expressed in terms of the r and θ components of the field by

$$E_z = E_r \cos\theta - E_\theta \sin\theta, \tag{98}$$

similarly to (61), from (35a),(35b), and (39) the field in the z direction incident on the nth dipole is given by

$$E_z^{0n} = \sum_{\substack{j=-\infty \\ j\neq n}}^{+\infty} b_j \frac{e^{ikd|j-n|}}{kd|j-n|}\left[\sin^2\theta_0 - \frac{i}{kd|j-n|}\left(2\cos^2\theta_0 - \sin^2\theta_0\right)\right.$$

$$\left. + \frac{1}{(kd)^2|j-n|^2}\left(2\cos^2\theta_0 - \sin^2\theta_0\right)\right], \quad n = 0, \pm 1, \pm 2, \ldots \pm\infty. \tag{99}$$

Now it is seen from (99) that if $\sin^2\theta_0 = 2\cos^2\theta_0$ or $\theta_0 = \arctan\sqrt{2} = \approx 54.74°$ then the higher-order distance terms vanish and we obtain

$$E_z^{0n} = \frac{2}{3}\sum_{\substack{j=-\infty \\ j\neq n}}^{+\infty} b_j \frac{e^{ikd|j-n|}}{kd|j-n|} \tag{100}$$

Inserting E_z^{0n} from (100) into (59), assuming the existence of a traveling wave (65), and letting $n = 0$ yields the equation similar to (67)

$$kd = \frac{2}{3}S_e \sum_{j=1}^{\infty}\left[\frac{e^{i(k+\beta)dj}}{j} + \frac{e^{i(k-\beta)dj}}{j}\right]. \tag{101}$$

Equation (101) is seen to be identical to [13, Eq.(59)], the equation for a linear periodic array of small isotropic electroacoustic transducers, with $2/3S_e$ instead of S_e. Hence we obtain directly

$$|S_e| = \frac{3}{2}\sin\psi_e, \quad kd < \beta d \tag{102}$$

and

$$\beta d = \cos^{-1}\left(-\frac{1}{2}e^{-kd\cot\psi_e} + \cos kd\right), \quad kd < \beta d. \tag{103}$$

Equation (103) gives an exact closed-form expression for the propagation constant β of the traveling wave supported by the linear periodic array of lossless, passive, small electric dipole antennas making an angle of $\theta_0 \approx 54.74°$ with the array axis, as a function of the normalized spacing kd of the dipoles and the phase ψ_e of the effective scattering coefficient. As $kd \to 0 \beta d \to \pi/3$ independent of ψ_e. Figure 15, taken from [13], contains curves of βd vs. kd for various values of ψ_e from 0° to 179°, and shows that there is at most one traveling wave for a given value of ψ_e and normalized spacing kd. Referring to Figure 5 which gives curves of ψ_e as a function of thin wire half-length for several different wire radii, we see that there are many different short wires that can be used to form a linear periodic array that

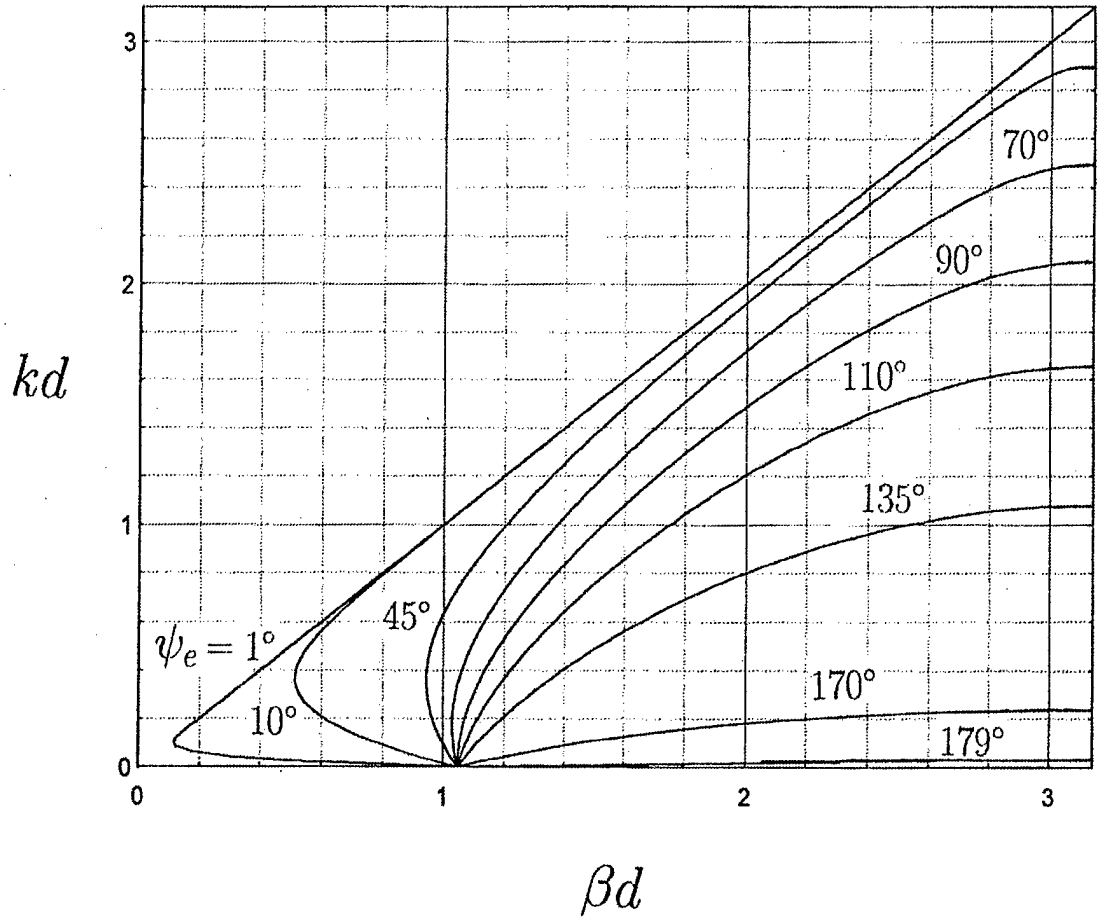

Figure 15: kd–βd curves for an infinite linear periodic array of short electric dipoles oriented at an angle $\theta_0 = 54.74°$ with respect to the array axis with different values of the phase ψ_e of the effective scattering coefficient.

will support a traveling wave. This conclusion is the opposite of that reached in the previous section when the thin wires were aligned with the array axis. Although the $kd - \beta d$ diagram for traveling waves supported by an infinite array of short dipoles making an angle of $\approx 54.74°$ with the array axis is identical to that for traveling waves supported by an infinite array of acoustic monopoles, the power ratio and directivity for a finite array of skewed electric dipoles are not the same as for an acoustic monopole array of the same number of elements because of the polarization of the dipoles. The equations to obtain the finite array coefficients are identical with [13, Eqs.(66)-(67)], that is (73)-(74) with the higher-order distance terms omitted, and the remainder of the analysis is the same as for the finite array of dipoles perpendicular to the array axis.

10 CONCLUDING REMARKS

A general vector spherical-wave source scattering-matrix description of an electromagnetic antenna has been formulated. Reciprocity and power conservation are applied to reduce the number of independent variables in the coefficients of the scattering matrix. The general formulation is then applied to a short z directed electric dipole antenna. While the vector spherical-wave harmonic source scattering-matrix formulation of a general electromagnetic antenna requires an expansion in an infinite number of vector spherical-wave harmonics, the electric field of a short z directed electric dipole antenna can be described with just the outgoing $\mathbf{N}_{10}^{(1)}(\mathbf{r})$ and incoming $\mathbf{N}_{10}^{(2)}(\mathbf{r})$ modes. The propagation constant of the traveling wave on a linear periodic array of short electric dipole antennas is shown to depend on just two parameters — the spacing (in wavelengths) kd of the radiators, and the phase ψ_e of the effective scattering coefficient of the radiators. Three orientations of the electric dipoles forming the array were considered: the electric dipoles perpendicular to the array axis, the dipoles aligned with the array axis, and the dipoles forming an angle $\theta_0 = \arctan\sqrt{2} \approx 54.74°$ with the array axis. A simple expression for the propagation constant β of the traveling wave was found in terms of kd and ψ_e in all three cases. When the dipoles are perpendicular to, or aligned with, the array axis the expression for the propagation constant is a transcendental equation which can be easily solved numerically. When the dipoles are oriented at an angle of $\theta_0 = \arctan\sqrt{2}$ with the array axis, a closed form expression for the propagation constant can be obtained that is identical to the expression that holds for the traveling wave on an array of acoustic monopoles. Curves of the functional dependence of βd on kd for different values of the phase of the effective scattering coefficient ψ_e are given for all three cases. For the perpendicular array, the relative phase velocity of the traveling wave calculated from the $kd - \beta d$ diagram using numerical values for the phase of the scattering coefficient for thin short wires obtained with the NEC scattering code are in close agreement with measurements made by Ehrenspeck and Poehler [1]. If the electric dipoles aligned with the array axis are simple short thin wires, the phases of the effective scattering coefficients obtained from the NEC code taken in combination with the corresponding $kd - \beta d$ diagram preclude the possibility any traveling waves being excited. For a Yagi-Uda finite array of N electric dipoles perpendicular to the array axis the two parameters kd and ψ_e are the only critical variables in the solution for the radiation coefficients.

Although the scattering-matrix analysis of arrays developed in this paper was applied only to arrays of short electric dipoles, the basic formulation applies to any array composed of linear, reciprocal, lossless array elements. A preliminary investigation suggests that an extension to arrays consisting of small spheres of a given permittivity and permeability is feasible. Such spheres can be described in terms of a pair of crossed electric and magnetic dipoles and would require four vector spherical wave function modes (two outgoing and two incoming) for their description. An extension to electrically larger array elements would require more spherical modes to represent their radiated and scattered fields, and thus more sophisticated procedures to obtain an efficient numerical solution for both infinite and finite arrays. In addition, it seems likely that the present analysis could be extended straightforwardly to two-dimensional linear arrays [30] and to arrays that do not lie in a straight line such as closed-loop traveling-wave arrays [12], and to surface or volumetric arrays of acoustic and electromagnetic radiators and scatterers (including small resonant scatterers) [10], [31]–[33].

A TRAVELING WAVE INEQUALITIES

Even though the inequalities in (1) are stated in a number of papers, texts, and antenna handbooks, we have not seen a proof of (1) for a general periodic array of electrically small elements. The second inequality in (1), namely, $\beta d \leq \pi$, follows from the fact that as βd becomes greater than π the traveling wave can merely be re-expressed as another traveling wave propagating in the negative z direction with a $\beta' d < \pi$. To see this, simply note that a periodic function that satisfies $p(x, y, z + d) = p(x, y, z)\mathrm{e}^{\mathrm{i}\beta d}$ with $\pi < \beta d < 2\pi$ also satisfies $p(x, y, z + d) = p(x, y, z)\mathrm{e}^{-\mathrm{i}\beta' d}$ with $0 < \beta' d = 2\pi - \beta d < \pi$, which is a wave traveling in the $-z$ direction. For $2\pi < \beta d \leq 3\pi$, the traveling wave can again be written as a wave propagating in the $+z$ direction with a propagation constant having a value less than π. For $3\pi < \beta d \leq 4\pi$, the traveling wave reverts to a wave propagating in the $-z$ direction with a propagation constant having a value less than π, and so on. Therefore, the full range of the absolute value of the propagation constant of any traveling wave can always be confined to a value equal to or less than π (see Footnote 1).

The first inequality in (1) implies that the traveling wave is a slow wave in that the phase velocity of the traveling wave is equal to or less than the speed of light. This first inequality can be proven for a general linear periodic array of lossless passive electrically small elements by looking at the radiation pattern of such an array as the number of elements in the array becomes infinite. The far-zone electric field $\mathbf{E}(\mathbf{r})$, radiated by a linear array consisting of an infinite number of identical antenna elements separated by a distance d from $z = -\infty$ to $z = +\infty$, such that each successive radiating element has the same complex far-zone electric field pattern $\boldsymbol{\mathcal{F}}(\theta, \phi)$ (which is proportional to the "embedded" element pattern) phase shifted by an amount $\mathrm{e}^{\mathrm{i}\beta d}$, is given by

$$\mathbf{E}(\mathbf{r}) \overset{r\to\infty}{\sim} \frac{\mathrm{e}^{\mathrm{i}kr}}{r}\boldsymbol{\mathcal{F}}(\theta, \phi)\left[\sum_{m=0}^{\infty} \mathrm{e}^{\mathrm{i}md(\beta+\mathrm{i}q_1-k\cos\theta)} + \sum_{m=0}^{\infty} \mathrm{e}^{-\mathrm{i}md(\beta-\mathrm{i}q_2-k\cos\theta)} - 1\right] \tag{104}$$

where θ is the spherical angle measured from the positive z axis. The far-field formula

used in (104) can be derived under the assumption that the sources are either confined to a finite region or decay exponentially at large distances from the origin. Thus, the small positive imaginary parts, iq_1 and iq_2, of β have been inserted into (104) to give the sources an exponential decay as z approaches plus and minus infinity, respectively. At the end of the derivation, q_1 and q_2 are allowed to approach zero.

Use of the summation formula, $\sum_{m=0}^{\infty} x^m = 1/(1-x)$, $|x| < 1$, converts (104) to

$$\mathbf{E}(\mathbf{r}) \overset{r\to\infty}{\sim} \frac{e^{ikr}}{r}\boldsymbol{\mathcal{F}}(\theta,\phi)\left[\frac{1}{1-e^{i(\beta-k\cos\theta)d}e^{-q_1}}+\frac{1}{1-e^{-i(\beta-k\cos\theta)d}e^{-q_2}}-1\right]. \tag{105}$$

In the limit as q_1 and q_2 approach zero, the quantity inside the square brackets of (105) equals 0 for $(\beta - k\cos\theta)d \neq 2n\pi$, and equals ∞ for $(\beta - k\cos\theta)d = 2n\pi$, $n = 0, \pm1, \pm2, \ldots \pm\infty$. However, the integration of the bracketed quantity in (105) with respect to the variable $u = (\beta - k\cos\theta)d$, over limits that cover just the singularity at $u = 0$, is equal to 4π as q_1 and q_2 approach zero. The same is true for limits of u that just cover the other singularities at $2n\pi$, $n = \pm1, \pm2, \ldots \pm\infty$. Therefore, as q_1 and q_2 approach zero, the bracketed quantity in (105) is simply an infinite sum of delta functions given by

$$\mathbf{E}(\mathbf{r}) \overset{r\to\infty}{\sim} 4\pi\frac{e^{ikr}}{r}\boldsymbol{\mathcal{F}}(\theta,\phi)\sum_{n=-\infty}^{\infty}\delta[(\beta-k\cos\theta)d-2n\pi]. \tag{106}$$

Each of the delta functions in (106) represent power radiated (actually an infinite amount of power radiated because the integral of the square of a delta function is infinite) by the array at the angles θ given by the zeroes of the arguments of the delta functions, provided the far-field pattern $\boldsymbol{\mathcal{F}}(\theta,\phi)$ does not have a null at these θ angles for all values of ϕ. The far-field pattern of small (nonresonant) antenna elements will contain no such nulls. Therefore, since a passive array carrying a lossless traveling wave cannot radiate and still maintain the traveling wave, for arrays of electrically small antenna elements, the arguments of the delta functions must not be zero for any θ other than $\theta = 0$, the direction of propagation of the traveling wave. In particular, if the argument of the $n = 0$ delta function cannot be zero for all $\theta \neq 0$, then $\beta \geq k$; that is, the traveling wave is a "slow" wave because its phase velocity is less than or equal to the speed of light. Also, (106) shows that there can be no traveling wave unless $kd \leq \pi$ even if βd is allowed to range from $-\infty$ to $+\infty$, provided again that there is no null in $\boldsymbol{\mathcal{F}}(\theta,\phi)$ at $\theta = \theta_0 > 0$ for all ϕ. If there is such a null, then a fast wave with $\beta d = kd\cos\theta_0$ may exist even if $kd > \pi$.

In all we have proven that

$$kd \leq \beta d \leq \pi \tag{107}$$

for a general infinite linear periodic array of lossless passive antenna elements for which there is no $\theta > 0$ such that $\boldsymbol{\mathcal{F}}(\theta,\phi) = 0$ for all ϕ — in particular, for electrically small (nonresonant) antenna elements. An analogous proof shows that the same inequalities apply also to the propagation constant of the traveling waves on linear periodic arrays of lossless passive transducer elements with no $\theta > 0$ such that the far-field element pattern $\mathcal{F}(\theta,\phi) = 0$ for all ϕ.

If the element pattern $\boldsymbol{\mathcal{F}}(\theta,\phi)$ of each antenna element does have a null at some $\theta = \theta_0 > 0$ for all ϕ, presumably a fast traveling wave with phase velocity greater than the speed of light

($\beta = k\cos\theta_0 < k$) that does not radiate can propagate along the array. If such an array were used as a scanning phased array antenna, the array antenna would have a "blind spot" at the scan angle equal to the null angle θ_0 of the element pattern [34]–[37].

As a conclusion to this appendix, we shall give an alternative proof that $\beta \geq k$ for far-field element patterns having no nulls with respect to $\theta > 0$. This alternative proof, which also reveals that traveling waves on a linear infinite periodic array must decay exponentially with radial distance from the axis of the array, begins by expanding the fields outside the elements of the array in terms of cylindrical waves. To avoid using vector cylindrical waves, assume an array of acoustic elements and express the acoustic pressure outside the elements carrying a traveling wave in a complete set of outgoing scalar cylindrical waves [22, ch. 6]

$$p(\rho,\phi,z) = \sum_{n=-\infty}^{+\infty} \int_{-\infty}^{+\infty} C_n(\gamma) H_n^{(1)}(\mathcal{K}\rho) \mathrm{e}^{\mathrm{i}n\phi} \mathrm{e}^{\mathrm{i}\gamma z} d\gamma \tag{108}$$

where the $H_n^{(1)}(\mathcal{K}\rho)$ are the cylindrical Hankel functions of the first kind and

$$\mathcal{K} = (k^2 - \gamma^2)^{\frac{1}{2}} \tag{109}$$

is chosen positive real or positive imaginary.

Applying the periodic boundary condition for the traveling wave

$$p(\rho,\phi,z+d) = p(\rho,\phi,z)\mathrm{e}^{\mathrm{i}\beta d} \tag{110}$$

and using orthogonality of the $\mathrm{e}^{\mathrm{i}n\phi}$ and $e^{i\gamma z}$ functions converts (108) to

$$p(\rho,\phi,z) = \sum_{n=-\infty}^{+\infty} \sum_{m=-\infty}^{+\infty} C_{nm} H_n^{(1)}(\mathcal{K}_m\rho) \mathrm{e}^{\mathrm{i}(\beta+2\pi m/d)z} \mathrm{e}^{\mathrm{i}n\phi} \tag{111}$$

with

$$\mathcal{K}_m = [k^2 - (\beta + 2\pi m/d)^2]^{\frac{1}{2}}. \tag{112}$$

The cylindrical modes in (111) are also the "Floquet modes" in the parallel plate waveguides of width d satisfying the periodic boundary condition (110).

The cylindrical far-field pattern (that is, the far-field pattern obtained by letting the length of the array approach infinity in the $\pm z$ directions before letting $\rho \to \infty$) can be found by replacing the Hankel functions in (111) by their large argument asymptotic forms to get

$$\sqrt{\rho}\, p(\rho,\phi,z) \overset{\rho\to\infty}{\sim} \sum_{m=-\infty}^{+\infty} C_m(\phi) \mathrm{e}^{\mathrm{i}[(\beta+2\pi m/d)z + \mathcal{K}_m\rho]} \tag{113}$$

in which

$$C_m(\phi) = \sqrt{\frac{2}{\pi\mathcal{K}_m}} \mathrm{e}^{-\mathrm{i}\pi/4} \sum_{n=-\infty}^{+\infty} (-\mathrm{i})^n C_{nm} \mathrm{e}^{\mathrm{i}n\phi}. \tag{114}$$

The cylindrical far-field pattern in (113) can be rewritten simply as

$$\sqrt{r\sin\theta}\, p(r,\theta,\phi) \overset{r\to\infty}{\sim} \sum_{m=-\infty}^{+\infty} C_m(\phi) \mathrm{e}^{\mathrm{i}kr\cos(\theta-\theta_m)} \tag{115}$$

where

$$\theta_m = \tan^{-1} \frac{\kappa_m}{\beta + 2\pi m/d}. \tag{116}$$

If θ_m is real, the mth mode in (115) represents a cylindrical wave propagating along a cone with half angle equal to θ_m. Thus, for (115) to represent the cylindrical far-field pattern of a nonradiating traveling wave, all the θ_m must be imaginary. That is, the κ_m must be imaginary for all nonzero $C_m(\phi)$. Now (115) also reveals that $C_m(\phi)$ cannot be zero for all ϕ unless $p(r, \theta, \phi)$ (defined by its analytic continuation if θ is complex) has no discrete cylindrical wave traveling in the direction $\theta = \theta_m$, or, equivalently, unless the far-field pattern of each element in the infinite array has a null at $\theta = \theta_m$ (for all ϕ). In any case, the cylindrical far field of a nonradiating traveling wave with $e^{i\beta z}$ dependence on a linear infinite periodic array decays exponentially with radial distance as

$$\frac{\exp\left[\mathrm{i}\beta z - \sqrt{(\beta + 2\pi m_1/d)^2 - k^2}\,\rho\right]}{\sqrt{\rho}} \tag{117}$$

as $\rho \to \infty$, where the integer m_1 is the index of the slowest exponentially decaying Floquet mode that is excited by the array elements.

Suppose the element far-field pattern has no nulls for real θ (and all ϕ) and $C_0 = 0$. Then if $\beta < k$, there must be a null in the far-field pattern for real θ (and all ϕ) since $C_0 = 0$. Consequently, if $C_0 = 0$ and the element far-field pattern has no nulls for real θ (and all ϕ), then $\beta \geq k$ and the only way that C_0 can be zero is for there to be a null at a complex value of θ (and all ϕ) in the analytically continued element far-field pattern.

B VECTOR SPHERICAL WAVE FUNCTIONS

In this Appendix we give the definitions of the vector spherical wave functions **M** and **N** used in this report. The definitions are those used by Billy Brock [16] adapted for the $\exp(-i\omega t)$ time dependence used here:

$$\mathbf{M}_{lm}^{(i)}(\mathbf{r}) = \mathrm{i}\sqrt{\frac{(2l+1)(l-m)!}{4\pi l(l+1)(l+m)!}} \begin{bmatrix} \dfrac{\mathrm{i}m}{\sin\theta} z_l^{(i)}(kr) P_l^m(\cos\theta) \mathrm{e}^{\mathrm{i}m\phi}\hat{\boldsymbol{\theta}} \\ \\ +\sin\theta z_n^{(i)}(kr) \dfrac{\mathrm{d}}{\mathrm{d}x} P_l^m(x)\Big|_{x=\cos\theta} \mathrm{e}^{\mathrm{i}m\phi}\hat{\boldsymbol{\phi}} \end{bmatrix}, \tag{118}$$

$$\mathbf{N}_{lm}^{(i)}(\mathbf{r}) = \mathrm{i}\sqrt{\frac{(2l+1)(l-m)!}{4\pi l(l+1)(l+m)!}} \begin{Bmatrix} \dfrac{z_l^{(i)}(kr)}{kr} l(l+1) P_l^m(\cos\theta) \mathrm{e}^{\mathrm{i}m\phi}\hat{\mathbf{r}} \\ \\ -\dfrac{1}{kr}\dfrac{\partial}{\partial r}\left[r z_l^{(i)}(kr)\right] \sin\theta \dfrac{\mathrm{d}}{\mathrm{d}x} P_l^m(x)\Big|_{x=\cos\theta} \mathrm{e}^{\mathrm{i}m\phi}\hat{\boldsymbol{\theta}} \\ \\ +\dfrac{1}{kr}\dfrac{\partial}{\partial r}\left[r z_l^{(i)}(kr)\right] \dfrac{\mathrm{i}m}{\sin\theta} P_l^m(\cos\theta) \mathrm{e}^{\mathrm{i}m\phi}\hat{\boldsymbol{\phi}} \end{Bmatrix}. \tag{119}$$

In (118) and (119) $z_l^{(1)}$ and $z_l^{(2)}$ are the spherical Bessel and Hankel functions j_l and $h_l^{(1)}$, respectively, and $P_l^m(x)$ is the associated Legendre function given by

$$P_l^m(x) = (-1)^m(1-x^2)^{m/2}\frac{\mathrm{d}^m}{\mathrm{d}x^m}P_l(x), m > 0, \tag{120a}$$

$$P_l^{-|m|}(x) = (-1)^m\frac{(n-m)!}{(n+m)!}P_l^m(x), m > 0, \tag{120b}$$

where $P_l(x)$ is the Legendre function

$$P_l(x) = \frac{1}{2^l l!}\frac{\mathrm{d}^l}{\mathrm{d}x^l}(x^2-1)^l. \tag{121}$$

The vector spherical wave functions $\mathbf{M}$ and $\mathbf{N}$ given by (118) and (119) can be defined in terms of the normalized radially-independent vector spherical harmonic function $\mathbf{X}_{lm}$ of Jackson [15] by

$$\mathbf{M}_{lm}^{(i)}(\mathbf{r}) \equiv z_l^{(i)}(kr)\mathbf{X}_{lm}(\theta,\phi) \tag{122}$$

and

$$\mathbf{N}_{lm}^{(i)}(\mathbf{r}) \equiv \frac{1}{k}\nabla \times z_l^{(i)}(kr)\mathbf{X}_{lm}(\theta,\phi), \tag{123}$$

and are related to the $\mathbf{F}_{1lm}^{(c)}$ and $\mathbf{F}_{2lm}^{(c)}$ vector spherical wave functions of Hansen [20] by

$$\mathbf{M}_{lm}^{(i)}(\mathbf{r}) = \mathrm{i}\mathbf{F}_{1ml}^{(c)}(\mathbf{r}) \tag{124}$$

and

$$\mathbf{N}_{lm}^{(i)}(\mathbf{r}) = \mathrm{i}\mathbf{F}_{2ml}^{(c)}(\mathbf{r})(\hat{\mathbf{r}}) \tag{125}$$

where the superscript $i = 1$ when $c = 1$ and the superscript $i = 2$ when $c = 3$.[3]

C SUMMATIONS OF TRIGONOMETRIC SERIES

In this Appendix we discuss the approximations used for the sums of the trigonometric series

$$F(a) \equiv \sum_{j=1}^{\infty}\frac{\sin na}{n^2}, 0 < a < \pi, \tag{126a}$$

and

$$G(a) \equiv \sum_{j=1}^{\infty}\frac{\cos na}{n^3}, 0 < a < \pi. \tag{126b}$$

Closed form expressions are not available for these sums. The IMSL least-squares approximation program FNLSQ was used to compute the approximations

$$F(a) \approx -0.1381\sin a + 0.03212\sin 2a - 0.9653a\ln(a/\pi), \quad 0 < a < \pi, \tag{127a}$$

[3]These relations between the vector spherical harmonics of Brock and those of Hansen are given incorrectly in the original form of [16] but have been corrected by Brock in an errata.

and

$$G(a) \approx 1.3328 - 0.1424\cos a + 0.01094\cos 2a + 0.4902a^2\ln(a/\pi) - 0.2417a^2, \quad 0 < a < \pi. \tag{127b}$$

Figures 16 and 17 show F(a) and G(a), respectively, calculated with 1000 terms, along with their least squares approximations. The agreement of the approximate with the exact curves is excellent. It will be noted that although $G'(a) = -F(a)$, when the approximation for $G(a)$ is differentiated the result differs slightly from the negative of the derivative of the approximation for $F(a)$. While it is possible to obtain an approximation for $F(a)$ by taking the negative of the derivative of the approximation for $G(a)$, the direct least-squares fit approximation for $F(a)$ that we have used distributes the errors in the approximation more uniformly over the interval from 0 to π.

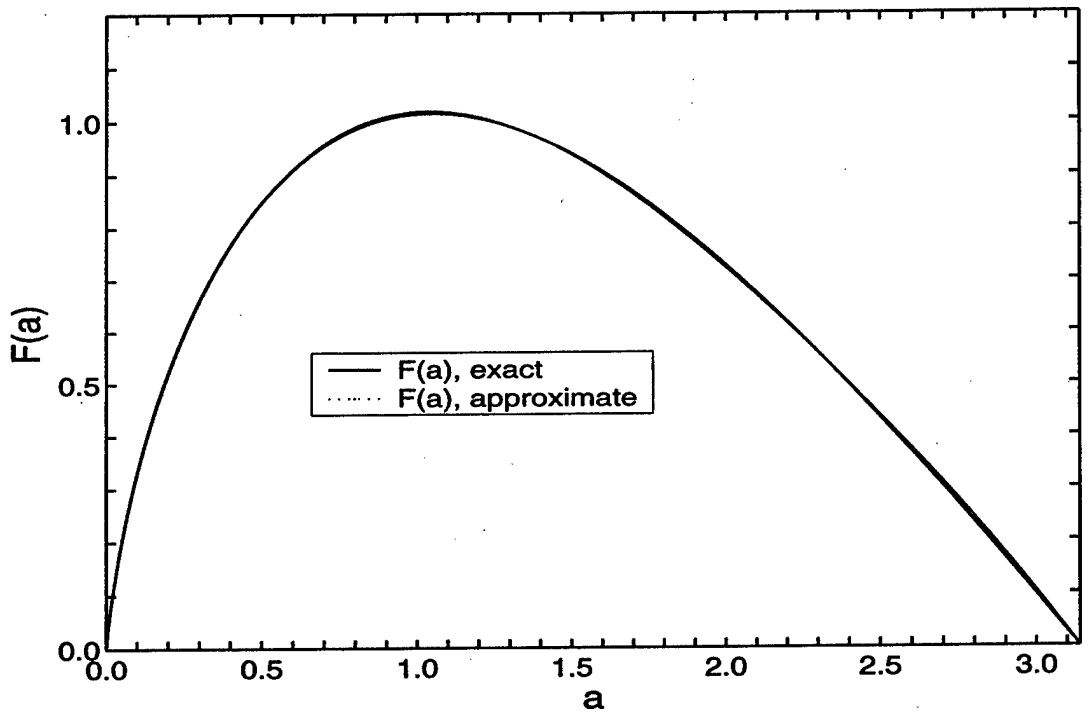

Figure 16: $F(a) \equiv \sum_{j=1}^{\infty} \frac{\sin na}{n^2}$, $0 < a < \pi$, exact and approximate.

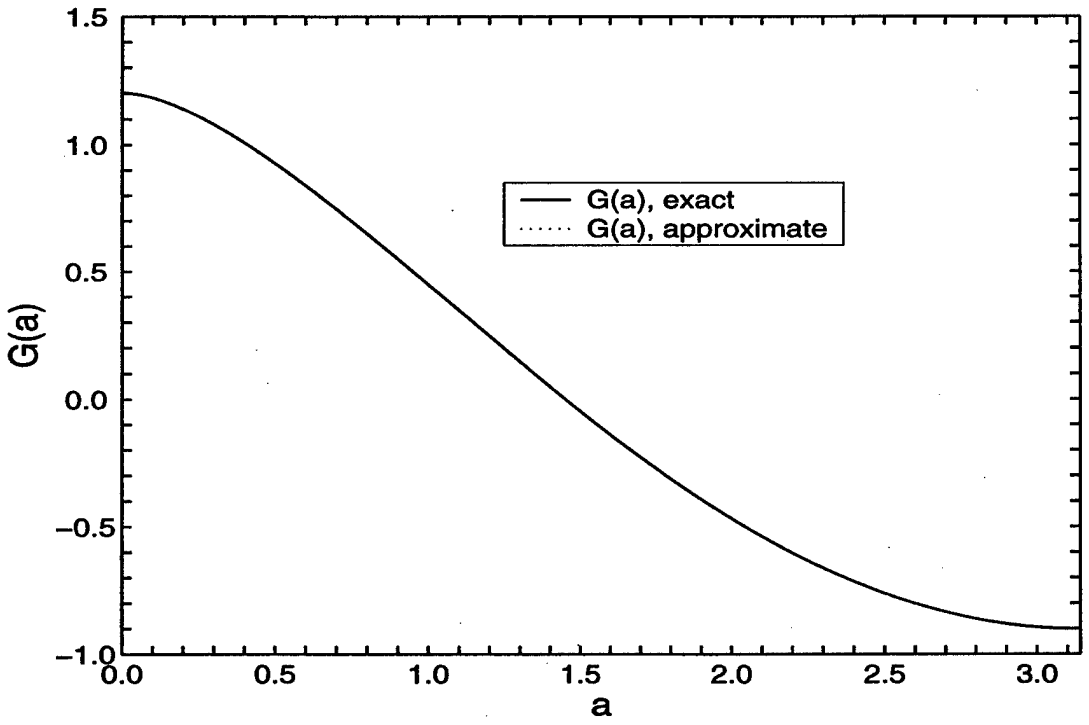

Figure 17: $G(a) \equiv \sum_{j=1}^{\infty} \frac{\cos na}{n^3}$, $0 < a < \pi$, exact and approximate.

References

[1] H.W. Ehrenspeck and H. Poehler, "A new method for obtaining maximum gain from Yagi antennas," *IRE Trans. Antennas Propagat.*, vol. AP-7, pp. 379–386, October 1959.

[2] D. L. Sengupta, "On the phase velocity of wave propagation along an infinite Yagi structure," *IRE Trans. Antennas Propagat.*, vol. AP-7, pp. 234–239, July 1959.

[3] R.J. Mailloux, "Antenna and wave theories of infinite Yagi-Uda arrays," *IEEE Trans. Antennas Propagat.*, vol. AP-13, pp. 499–506, July 1965.

[4] R.J. Mailloux, "Excitation of a surface wave along an infinite Yagi-Uda array," *IEEE Trans. Antennas Propagat.*, vol. AP-13, pp. 719–724, September 1965.

[5] R.J. Mailloux, "The long Yagi-Uda array," *IEEE Trans. Antennas Propagat.*, vol. AP-14, pp. 128–137, March 1966.

[6] C.H. Walter, *Traveling Wave Antennas*, McGraw-Hill, New York, 1965.

[7] A. Hessel, "General Characteristics of Traveling-wave Antennas," ch. 19 in *Antenna Theory, Part 2*, Eds. R.E. Collin and F.J. Zucker, New York: McGraw-Hill, 1969. 050–1064, August 2002.

[8] A.D. Yaghjian and E.T. Kornhauser, "A modal analysis of the dielectric rod antenna excited by the HE_{11} mode," *IEEE Trans. Antennas Propagat.*, vol. AP-20, pp. 122–128, March 1972.

[9] A.D. Yaghjian, "Approximate formulas for the far field and gain of open-ended rectangular waveguide," *IEEE Trans. Antennas Propagat.*, vol. AP-32, pp. 378–384, April 1984.

[10] V.V. Veremey and R. Mittra, "Scattering from structures formed by resonant elements," *IEEE Trans. Antennas Propagat.*, vol. 46, pp. 494–501, April 1998.

[11] F. Serracchioli and C.A. Levis, "The calculated phase velocity of long end-fire uniform dipole arrays," *IRE Trans. Antennas Propagat.* (Special Supplement), vol. AP-7, pp. S424–S434, December 1959.

[12] G. Fikioris, "Field patterns of resonant noncircular closed-loop arrays," *J. Electromagnetic Waves and Applications*, vol. 10, no. 3, pp. 307–327, 1996.

[13] A.D. Yaghjian, "Scattering-Matrix Analysis of Linear Periodic Arrays," *IEEE Trans. Antennas Propagat.*, vol. 50, pp. 1050-1064, August 2002.

[14] W.W. Hansen and J.R. Woodyard, "A new principle in directional antenna design," *Proc. IRE*, vol. 26, pp. 333–345, March 1938.

[15] J.D. Jackson, *Classical Electrodynamics, 3rd Edition*, New York: Wiley, 1999.

[16] B.C. Brock, *Using Vector Spherical Harmonics to Compute Antenna Mutual Impedance from Measured or Computed Fields*, Sandia Report SAND2000-2217, Sandia National Laboratories, September, 2000. Available on the web at http://www.prod.sandia.gov/cgi-bin/techlib/access-control.pl/2000/002217r.pdf

[17] A.D. Yaghjian, *Near-Field Measurements on a Cylindrical Surface: A Source Scattering-Matrix Formulation*, NBS Technical Note 696, Boulder, CO, September 1977.

[18] J. Appel-Hansen, E.S. Gillespie, T.G. Hickman, and J.D. Dyson, "Antenna Measurements," ch. 8 in *The Antenna Design Handbook, Vol. 1*, Eds. A.W. Rudge, K. Milne, A.D. Olver, and P. Knight, London: Peregrinus, 1982.

[19] C.G. Montgomery and R.H. Dicke, "Waveguide Junctions with Several Arms," ch. 9 in *Principles of Microwave Circuits*, Eds. C.G. Montgomery, R.H. Dicke, and E.M. Purcell, New York: McGraw-Hill, 1948.

[20] J.E. Hansen, Ed., *Spherical Near-Field Antenna Measurements*, London: Peregrinus, 1988.

[21] R.E. Collin and F.J. Zucker, *Antenna Theory, Part 1*, New York: McGraw-Hill, 1969.

[22] J.A. Stratton, *Electromagnetic Theory*, New York: McGraw-Hill, 1941.

[23] E.M. Purcell and C.R. Pennypacker, "Scattering and absorption of light by nonspherical dielectric grains," *Astrophysical Journal*, vol. 186, pp. 705–714, 1 December 1973.

[24] B.T. Draine, "The discrete-dipole approximation and its application to interstellar graphite grains," *Astrophysical Journal*, vol. 333, pp. 848–872, 15 October 1988.

[25] I.S. Gradshteyn and I.M. Ryzhik, *Table of Integrals, Series, and Products; 5th Edition*, Boston: Academic, 1994.

[26] G.J. Burke and A.K. Poffio, "Numerical Electromagnetics Code (NEC) - Method of Moments," Report UCIZ 18834, Lawrence Livermore Laboratory, CA, January 1981.

[27] J.M. Putnam and L.N. Medgyesi-Mitschang, *Combined Field Integral Equation Formulation for Axially Inhomogeneous Bodies of Revolution*, McDonnell Douglas Research Laboratories MDC Report No. QA003, December 1987.

[28] H. Bach and J.E. Hansen, "Uniformly Spaced Arrays," ch. 5 in *Antenna Theory, Part 1*, Eds. R.E. Collin and F.J. Zucker, New York: McGraw-Hill, 1969.

[29] W.K. Kahn, "Currents on Generalized Yagi Structures," *IEEE Trans. Antennas Propagat.*, vol. AP-27, pp. 788–797, November 1979.

[30] L. Carin and L.B. Felsen, "Time harmonic and transient scattering by finite periodic flat strip arrays: hybrid (ray)-(Floquet mode)-(MOM) algorithm," *IEEE Trans. Antennas Propagat.*, vol. 41, pp. 412–421, April 1993.

[31] J.B. Pendry, A.J. Holden, D.J. Robbins, and W.J. Stewart, "Magnetism from conductors and enhanced nonlinear phenomena," *IEEE Trans. MTT*, vol. 47, pp. 2075–2084, November 1999.

[32] D. Sievenpiper, L. Zhang, R.F.J. Broas, N.G. Alexópolous, and E. Yablonovitch, "High-impedance electromagnetic surfaces with a forbidden frequency band," *IEEE Trans. MTT*, vol. 47, pp. 2059–2074, November, 1999.

[33] D.R. Smith, W.J. Padilla, D.C. Vier, S.C. Nemat-Nasser, and S. Schultz, "Composite medium with simultaneously negative permeability and permittivity," *Physical Review Letters*, vol. 84, pp. 4184–4187, 1 May 2000.

[34] C.P. Wu and V. Galindo, "Surface-wave effects on dielectric sheathed phased arrays of rectangular waveguides," *Bell System Tech. J.*, vol. 47, pp. 117-142, January 1968.

[35] G.H. Knittel, A. Hessel, A.A. Oliner, "Element pattern nulls in phased arrays and their relation to guided waves," *Proc. IEEE*, vol. 56, pp. 1822–1836, November 1968.

[36] G.V. Borgiotti, "Modal analysis of periodic planar phased arrays of apertures," *Proc. IEEE*, vol. 56, pp. 1881–1892, November 1968.

[37] R.J. Mailloux, "Surface waves and anomalous wave radiation nulls on phased arrays of TEM waveguides with fences," *IEEE Trans. Antennas Propagat.*, vol. AP-20, pp. 160–166, March 1972.